Nuclear Physics B366 (1991) 135–188
North-Holland

NUCLEAR
PHYSICS B

HIGH ENERGY FACTORIZATION AND SMALL-x HEAVY FLAVOUR PRODUCTION*

S. CATANI

Cavendish Laboratory, University of Cambridge, Cambridge, UK
and
INFN, Sezione di Firenze, Firenze, Italy

M. CIAFALONI and F. HAUTMANN

Dipartimento di Fisica, Universitá di Firenze
and
INFN, Sezione di Firenze, Firenze, Italy

Received 4 February 1991
(Revised 15 April 1991)

We have recently proposed a form of high-energy factorization in order to find the small-x behaviour of heavy mass production in QCD. This factorization is $k_\perp$-dependent and provides all leading ln x corrections to the coefficient function in various kinds of single-$k_\perp$ and double-$k_\perp$ processes. Here we investigate in detail its application to heavy flavour production in lepton and hadron initiated processes. We find that the resummation procedure yields large correction factors with respect to the lowest-order result, and we compute their explicit form in various cases.

1. Introduction

Heavy flavour physics has long been considered as an ideal framework for perturbative QCD, due to the smallness of the running coupling constant $\alpha_s(M^2) = (b \ln M^2/\Lambda^2)^{-1}$ when the quark mass M is much larger than the QCD scale Λ. However in the TeV energy range, or higher, which is to be considered with the new colliders, heavy flavour production enters a two-scale regime in which the energy $S \gg M^2 \gg \Lambda^2$. In such a case QCD perturbation theory is affected by large coefficients, which are $O(\ln^m S/M^2)$, besides the usual ones, predicted by the renormalization group, which are $O(\ln^n M^2/\Lambda^2)$.

* Research supported in part by the UK Science and Engineering Research Council and in part by the Italian Ministero della Pubblica Istruzione.

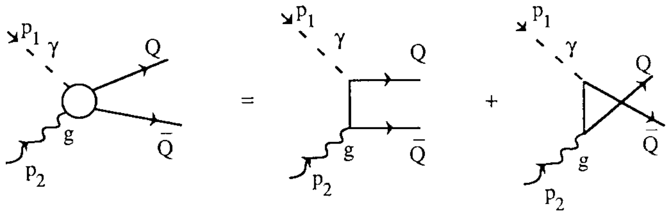

Fig. 1. Feynman diagrams for heavy flavour photoproduction at the Born level.

The first perturbative corrections to the basic photo- and hadro-production diagrams have been analyzed in detail in the literature [1–3]. For instance, in the photo-production case, the Born cross section σ_{Born} (fig. 1) and its first order correction $\sigma_{1\text{-loop}}$ are

$$4M^2\sigma_{\gamma g,\,\mathrm{Born}}(\rho) = 2\pi\alpha\alpha_s e_Q^2 \int_\rho^1 \frac{d\xi}{\sqrt{1-\xi}}\frac{\rho}{\xi}\left(1-\tfrac{1}{2}\xi+\rho-\frac{\rho^2}{\xi}\right)$$

$$= 2\pi\alpha\alpha_s e_Q^2 \rho\beta\left[\left(1+\rho-\tfrac{1}{2}\rho^2\right)\mathscr{L}(\beta)-1-\rho\right], \qquad (1.1)$$

$$4M^2\sigma_{\gamma g,\,1\text{-loop}}(\rho, M^2/Q_0^2) = \alpha\alpha_s^2(M^2)\left[c_1(\rho)+\bar{c}_1(\rho)\ln M^2/Q_0^2\right], \qquad (1.2)$$

where

$$\rho = 4M^2/S, \qquad \beta = \sqrt{1-\rho}\,, \qquad (1.3)$$

$$\mathscr{L}(\beta) = \frac{1}{\beta}\ln\frac{1+\beta}{1-\beta}, \qquad (1.4)$$

and, for $\rho \to 0$ ($S \gg M^2$), one has the constant limits

$$c_1 = \tfrac{164}{27}C_A e_Q^2, \qquad \bar{c}_1 = \tfrac{28}{9}C_A e_Q^2. \qquad (1.5)$$

Here α is the fine structure constant, e_Q is the heavy flavour charge, $C_A = N_c$ is the number of colours and Q_0 is the factorization scale (such that $\alpha_s(Q_0^2) \leqslant 1$).

Note that $\sigma_{1\text{-loop}}$, due to eq. (1.5), is asymptotically constant, as expected from gluon exchange (fig. 2a), while $\sigma_{\mathrm{Born}} \sim \rho\ln(1/\rho)$ is vanishingly small, consistently with fermion exchange (fig. 1). This constant behaviour of $\sigma_{1\text{-loop}}$ will generate, at higher orders, powers of $\ln\rho$ which are not necessarily associated with powers of $\ln M^2/Q_0^2$, thus affecting also the coefficient factor.

The modifications of the anomalous dimension due to the powers of $\ln\rho$ is well-known [4], and can be traced back to the work of Lipatov and collaborators [5] which has been recast in various forms later on [6–8]. In the leading $\ln S/M^2$

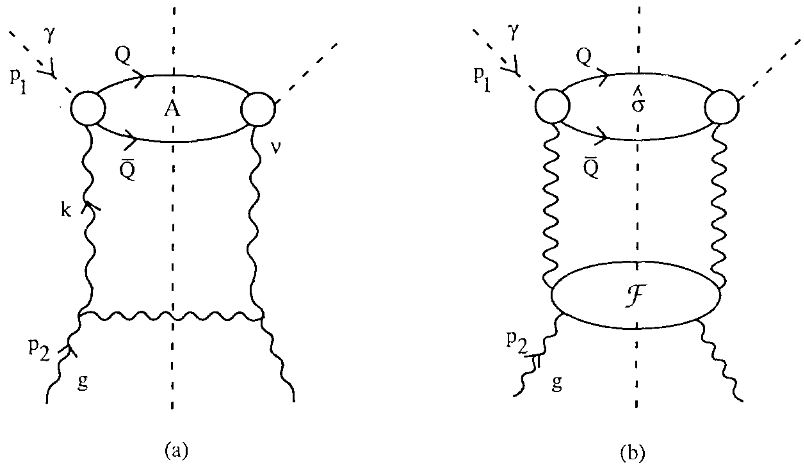

Fig. 2. Heavy flavour photo-production at high-energy: (a) one loop correction to the Born approximation and (b) factorized structure of the cross section in the Regge limit.

approximation (LLA) the anomalous dimension γ_N turns out to be a function of $\bar{\alpha}_s/N$, where $\bar{\alpha}_s = 3\alpha_s/\pi$ and N is the moment index. For very small values of $\bar{\alpha}_s/N$, i.e. in the perturbative regime, one has the expression

$$\gamma_N(\alpha_s) = \frac{\bar{\alpha}_s}{N} + 2\zeta(3)\left(\frac{\bar{\alpha}_s}{N}\right)^4 + \dots, \tag{1.6}$$

which departs rather slowly from the one-loop value of the Altarelli–Parisi equation. Note however that for sizeable values of $\bar{\alpha}_s/N \sim \mathrm{O}(1)$, γ_N increases instead quite fast, reaching [5] the saturating value $\gamma_N = 1/2$ for $\bar{\alpha}_s/N = (4\ln 2)^{-1}$ (see sect. 2).

This behaviour of the anomalous dimension is of course universal, and is expected to hold in the heavy flavour case too, possibly affected by unitarizations corrections [9, 10] at extreme energies. On the other hand, the large $\ln\rho$ terms affect also the coefficient factor, which is process-dependent and whose perturbative expansion does not seem to follow any simple rule.

The purpose of this paper is to show that actually all leading logs of the coefficient factor can be evaluated and (in some cases) resummed in closed form. Part of these results have been anticipated in short notes [11, 12]. Here we provide a complete account of the photo- and lepto-production cases and the main ingredients for dealing with hadro-production processes.

The basic idea of our approach, proposed in ref. [11], is to replace the collinear (or parton pole) factorization of hard vertex cross section and structure function with the corresponding high-energy (or gluon Regge pole) factorization which is

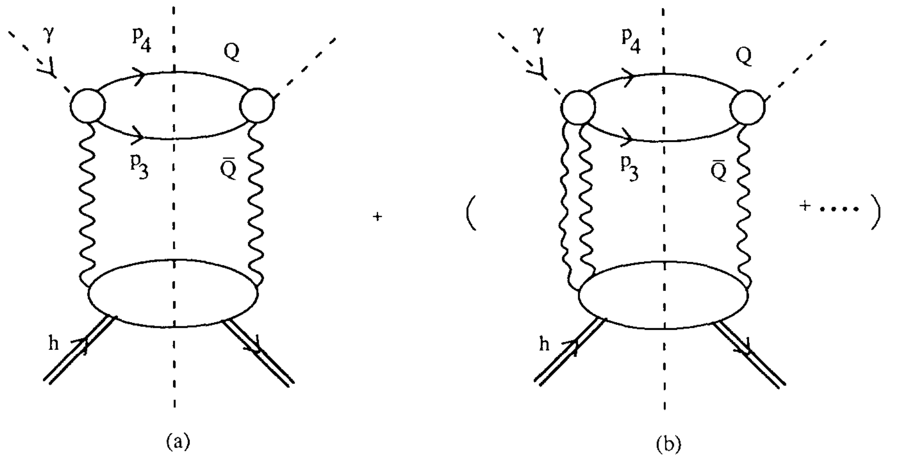

Fig. 3. (a) Single and (b) multiple Regge-gluon exchanges for photo-production in the high-energy limit.

$k_\perp$-dependent (fig. 3a). The latter reduces to the former for $S \gg M^2 \gg k_\perp^2$, but holds also for $S \gg M^2 \sim k_\perp^2$, i.e. for any value of $k_\perp/M$. Since the large factors $(\ln \rho)^k$ (or $(\alpha_s/N)^k$ in momentum space) are generated in the coefficient function by $k_\perp$-integration from the ones in the anomalous dimension, we are able to evaluate and resum them.

The high-energy factorization formulas used here are valid in LLA because they involve single t-channel Regge exchanges. Multiple Regge-gluon exchanges (fig. 3b) are not factorized, but are suppressed by powers of $\alpha_s(M^2)$. Our procedure applies to various kinds of single-$k_\perp$ and double-$k_\perp$ hard processes. Among the ones we treat, heavy flavour photo-production involves the single-$k_\perp$ hard subprocess $\gamma + g(k_\perp) \to Q\bar{Q}$, while lepto-production and hadro-production involve two high-energy exchanges and momentum transfers $k_{\perp 1}, k_{\perp 2}$.

In more detail, the factorization procedure involves two steps: (i) computing the $\gamma^*(k_{\perp 1}) + g^*(k_{\perp 2}) \to Q\bar{Q}$ or $g^*(k_{\perp 1}) + g^*(k_{\perp 2}) \to Q\bar{Q}$ Born cross section for the conversion of the off-shell gluons (photons) exchanged at high energies, and (ii) performing a convolution with the gluon structure function(s) including small-x corrections.

While the energy dependence is essentially due to the structure function evaluation of the second step, the coefficient factor comes out from the $k_\perp$-integrations in the first one. This integration, which has been performed analytically in some cases, is by no means a trivial effect. In fact, it provides eventually a large K-factor, which is asymptotically of order 5 for photo-production, and is logarithmically increasing for hadro-production.

The presence of such large coefficients raises the obvious question of the convergence of such resummation, which is within the logic of LLA, i.e. neglects terms which are of relative order $\alpha_s(M^2)$. We can only say that we expect in this case the same range of validity of the Regge expansion in large-$k_\perp$ physics, which is also at the basis of the small-x behaviour of the gluon structure function.

The outline of the paper is as follows. In sect. 2 we justify and we write in detail the factorization formula for the case of photo-production. In sect. 3 we perform the ensuing convolution and we discuss its high-energy behaviour in the perturbative regime (small $\bar{\alpha}_s/N$) and at extreme energies (i.e. when the anomalous dimension saturates at $\gamma = 1/2$). We also obtain the values of the K-factors for both regimes. In sect. 4 we discuss in detail the lepto-production case, which is the simplest double-$k_\perp$ process, and we obtain explicit formulas for the resummed K-factors and their Q^2/M^2 dependence. In sect. 5 we introduce the factorization formula for the hadro-production case and we discuss the convolution procedure, that we explicitly perform for the abelian diagrams only. The qualitative behaviour of the cross section at high energies and its distinctive features are also discussed. The result obtained are summarized in sect. 6 where we also discuss their range of applicability and their physical content.

A few mathematical details of the kinematics and of the Feynman diagrams calculations are left to appendices A to C. In particular in appendix B we give the single-$k_\perp$ and double-$k_\perp$ matrix elements for the hard vertex cross sections (both abelian and non-abelian ones) and in appendix C we calculate their $k_\perp$-moments.

2. High-energy factorization. The photo-production case

Consider the photo-production process (fig. 3)

$$\gamma(p_1) + \mathrm{h}(p_2) \to \overline{\mathrm{Q}}(p_3) + \mathrm{Q}(p_4) + \mathrm{X} \tag{2.1}$$

in the high-energy limit

$$S \simeq 2p_1 \cdot p_2 \gg M^2 = p_3^2 = p_4^2 \gg \Lambda^2. \tag{2.2}$$

The cross section behaviour at large $S \gg 4M^2$ (or $\rho = 4M^2/S \to 0$) is perturbatively quasi-constant (i.e. it is a sum of powers of logs) because of the spin-one gluon exchange (fig. 2a) and of its t-channel (fig. 3a) and s-channel (fig. 3b) iteration.

The QCD treatment of this process (which is not genuinely hard) is supposed [13] to be perturbative because of the large scale M^2 (such that $\alpha_s(M^2) \ll 1$) and of the typically large value of the exchanged transverse momentum $k_\perp \sim \mathrm{O(M)}$. However, at very high energies, such that $S \gg k_\perp^2 \sim M^2 \gg \Lambda^2$, one enters a two-scale regime where powers of $\ln S/M^2$ are generated both in the anomalous dimension and in the coefficient function of the process (2.1), as discussed in sect. 1. In the following, we shall show that the resummation of such large logs in the

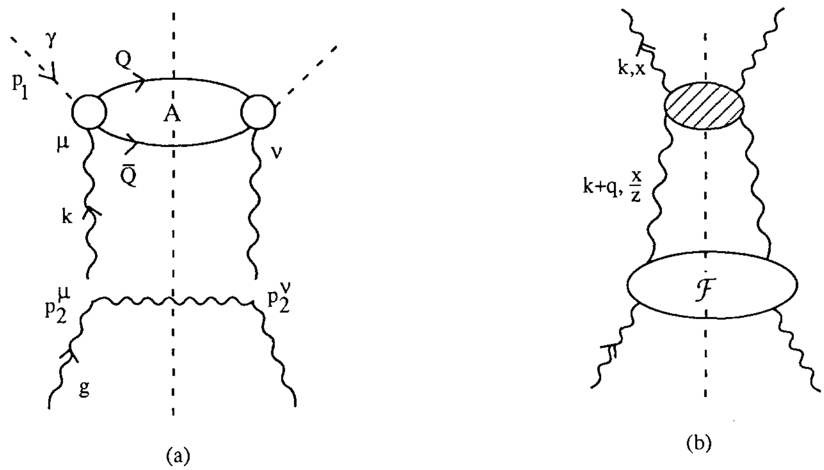

Fig. 4. (a) Hard vertex cross section for photo-production and (b) iteration kernel for the Lipatov equation.

coefficient part follows from the one in the anomalous-dimension part in virtue of a factorization property which is valid at high energies and supplements the one due to the renormalization group [13].

In the two-scale, high-energy regime just mentioned, we want to establish the following factorization formula, for the gluon–photon total cross section (fig. 2b)

$$4M^2\sigma_{\gamma g}(\rho, M^2/Q_0^2) = \int d^2\mathbf{k} \int_0^1 \frac{dz}{z} \hat{\sigma}(\rho/z, \mathbf{k}^2/M^2) \mathscr{F}(z, \mathbf{k}; Q_0^2). \quad (2.3)$$

Here $\mathscr{F}(x, \mathbf{k})$ is the unintegrated gluon structure function defined below (fig. 4b), and $\hat{\sigma}$ is the off-shell $\gamma + g(k) \to Q\overline{Q}$ Born cross section, defined by coupling the external gluon to high-energy partons by eikonal vertices (fig. 4a).

Eq. (2.3) states that a t-channel exchange of a (Regge) gluon of virtualness $k^2 \simeq -k_\perp^2$ dominates the process (2.1) in the high-energy limit

$$(p_1 + p_2)^2 \equiv S \gg (p_3 + p_4)^2, (p_2 - k)^2. \quad (2.4)$$

However it also states that in this limit the vertex factor $\hat{\sigma}$ and $\mathscr{F}$ (which are, not surprisingly, $k_\perp$-dependent) are well defined and calculable in the LLA as explained below.

In order to prove eq. (2.3), we shall rely heavily on the analysis of the multi-Regge behaviour of Yang–Mills theories pioneered in ref. [5] and of the related particle production given in ref. [7]. According to this analysis, many-gluon exchanges iterated in the s-channel (fig. 3b) are sub-leading in a physical gauge $A \cdot n = 0$ by at least one power of $\alpha_s(M^2)$, while the diagrams providing leading logarithms of S/M^2 are given by multiple t-channel gluon exchanges, which define a generalized ladder. In fig. 2b we have singled out the upper rung of such ladder, corresponding to an exchanged gluon of momentum k, and embodied the remaining ones in $\mathscr{F}$. Furthermore, the dominant integration region in the k-variable

$$k^{\mu} = zp_2^{\mu} + k_{\perp}^{\mu} + \frac{k^2 + \mathbf{k}^2}{zS} p_1^{\mu}, \tag{2.5}$$

was shown to be the one of fixed $k_{\perp}$, small z and $k^2 \simeq -k_{\perp}^2$, or more precisely

$$\frac{k^2 + \mathbf{k}^2}{zS} = \mathrm{O}\left(\frac{k_{\perp}^2}{S}\right) \ll 1. \tag{2.6}$$

On the other hand, $k_{\perp}^2/zS$ (or $k_{\perp}^2/(p_3+p_4)^2$) are, in this regime, variables of order unity (cf. appendix A for the kinematical details).

After these premises, we need only to show that a single gluon polarization contributes to the diagram in fig. 2b, providing precise definitions for the off-shell $\mathrm{Q\overline{Q}}$ cross section $\hat{\sigma}$ and for $\mathscr{F}$. Let $A_{\mu\nu}$ denote the lowest-order $\mathrm{Q\overline{Q}}$ contribution to the $\gamma \mathrm{g} \to \gamma \mathrm{g}$ absorptive part (fig. 4a), and let $G_{\mu\nu}$ be the full $\mathrm{gg} \to \mathrm{gg}$ absorptive part, including the gluon propagator, computed in the axial gauge with $n = p_1$. Then the cross section in fig. 2b can be written as

$$\sigma_{\gamma \mathrm{g}} = \frac{1}{2S} \int \frac{\mathrm{d}^4 k}{(2\pi)^4} A_{\mu\nu}(p_1, k) G^{\mu\nu}(p_2, k), \tag{2.7}$$

where the physical polarization sum $d^{\mu\nu}(k)$ in the μ and ν indices has been dropped, due to the fact that, in this single $k_{\perp}$ case*, the "currents" $A_{\mu\nu}$ and $G_{\mu\nu}$ are conserved.

We then note that the lowest-order abelian absorptive part $A_{\mu\nu}$ is independent of the gauge vector and has therefore the invariant decomposition

$$A^{\mu\nu}(p_1, k) = A_1\left(-g^{\mu\nu} + \frac{k^{\mu}k^{\nu}}{k^2}\right) - \frac{1}{k^2} A_2 \left(\frac{k^2}{p_1 k} p_1^{\mu} - k^{\mu}\right)\left(\frac{k^2}{p_1 k} p_1^{\nu} - k^{\nu}\right), \tag{2.8}$$

where A_1 and A_2 are functions of the rescaled variables ρ/z and k^2/zS

$$A_1 = A_1(\rho/z, k^2/zS), \qquad A_2 = A_2(\rho/z, k^2/zS), \tag{2.9}$$

and can be explicitly computed (cf. eq. (B.21) for A_2).

* One could as well incorporate the $d_{\mu\nu}(k)$ factors (in the gauge $A \cdot n = 0$) into $A_{\mu\nu}$, as done for the double $k_{\perp}$ non-abelian case in appendix B, with the same final result.

We want to show that, in the kinematical region for k^μ described above, the A_2 term provides the dominant high-energy contribution to eq. (2.7), due to its enhancing polarization factor.

Note first that in the high-energy regime ($\rho \to 0$) A_1 and A_2 themselves are both small and of the same order, $A_1 \sim A_2 \sim O(\rho/z)$ for fixed values of k^2/zS. This is due to the fact that they are given by spin-1/2 exchange diagrams, and is easily verified by explicit calculation, along the lines of appendix C. Finally, let us note that A_1 and A_2 must coincide on-shell ($k^2=0$)

$$A_1(\rho/z, k^2=0) = A_2(\rho/z, k^2=0), \tag{2.10}$$

in order to cancel the spurious $k^2=0$ pole of eq. (2.8). Thus on-shell we have

$$2zS\sigma_{\gamma g,\,\mathrm{Born}} = -A_\mu{}^\mu = (3A_1 - A_2) = 2A_2 \qquad (\text{for} \quad k^2=0). \tag{2.11}$$

Since A_1 and A_2 are both small and of the same order for $\rho/z \to 0$, the dominant high-energy behaviour of (2.7) is obtained for fixed values of $\rho/z \sim O(1)$ (and thus $z \to 0$) and will come out to be a constant, up to logarithms, as expected from gluon exchange. On the other hand, for $z \to 0$, $k^2 \simeq -k_\perp^2$ and k^2/zS fixed, the polarization factor in front of A_2 in eq. (2.8) can be replaced by

$$\frac{4\mathbf{k}^2}{zS}\frac{p_1^\mu p_1^\nu}{S}\frac{1}{z}\left[1 + O\left(z, \mathbf{k}/\sqrt{S}\right)\right] \tag{2.12}$$

and thus provides a net $1/z$ enhancement factor over the A_1 term. Therefore the polarization factor singles out A_2 at high energies, by leading to complete factorization of vertex and structure function terms. In a different language, this comes from factorization at the t-channel angular momentum pole of the $J=1$ exchanged gluon. For this reason we have referred to it as due to (Regge) gluon exchange.

To sum up, in the high-energy regime of eqs. (2.4)–(2.6) we obtain

$$\int \frac{\mathrm{d}k^2}{2(2\pi)^4} A_{\mu\nu} G^{\mu\nu} \simeq \int \frac{\mathrm{d}k^2}{2(2\pi)^4} \frac{4\mathbf{k}^2}{z^2 S^2} A_2 p_1^\mu p_1^\nu G_{\mu\nu}$$

$$= \frac{S}{2M^2} \hat{\sigma}(\rho/z, \mathbf{k}^2/M^2) \mathscr{F}(z, \mathbf{k}), \tag{2.13}$$

where we have defined

$$\mathscr{F}(z, \mathbf{k}) \equiv \int \frac{\mathrm{d}k^2}{(2\pi)^4} \frac{\mathbf{k}^2}{zS^2} p_1^\mu p_1^\nu G_{\mu\nu}, \tag{2.14}$$

with $G_{\mu\nu}$ evaluated in the $n=p_1$ gauge, and

$$\hat{\sigma} \equiv \frac{\rho}{z} A_2 \simeq \frac{\rho}{z} \frac{z^2}{\mathbf{k}^2} p_2^\mu p_2^\nu A_{\mu\nu} . \tag{2.15}$$

By substituting (2.13) into (2.7), eq. (2.3) follows.

Our derivation shows that $\hat{\sigma}$ in eq. (2.15) is "measured" by the physical process in fig. 4a in the high-energy limit (2.4). This is because, in this limit, the external parton couples to the exchanged soft gluon ($z \to 0$) with an eikonal vertex, as obtained in eq. (2.15). Furthermore, by eq. (2.11), $\hat{\sigma}$ reduces on-shell ($k_\perp^2 \to 0$) to the $\gamma g \to Q\overline{Q}$ Born cross section. Therefore $\hat{\sigma}$ is the off-shell continuation of σ_{Born} defined by the Regge limit of a physical process and is thus in general gauge invariant (cf. Appendix B).

Let us note that, if the $k_\perp$-integration in eq. (2.3) were restricted to its lower corner ($k_\perp^2 \ll M^2$), then the naive renormalization group factorization formula would be valid. In fact $\hat{\sigma}$ would reduce to σ_{Born} and $\mathscr{F}$ would be integrated up to M^2. Thus the extra dynamical information contained in eq. (2.3) lies in the high-energy factorization of $\hat{\sigma}(k_\perp)$ and in its $k_\perp$ dependence for $k_\perp/M \sim O(1)$, or higher. In this sense, eq. (2.3) is a generalization of the usual renormalization group factorization theorem away from the collinear pole.

The definition in eq. (2.14) yields the second ingredient of eq. (2.3), i.e. the unintegrated gluon structure function $\mathscr{F}$, which embodies all gluon t-channel exchanges exemplified in fig. 2b and worked out by Fadin, Kuraev, Lipatov and collaborators in ref. [5]. In this paper, where we are mostly concerned with the coefficient function related to $\hat{\sigma}$, we shall work at parton level for the structure function. Thus, following refs. [4–9] we define the unintegrated structure function of a gluon of virtualness $-k^2 \simeq \mathbf{k}^2 = Q_0^2$ by the integral equation (fig. 4b)

$$\mathscr{F}(x,\mathbf{k};Q_0^2) = \frac{1}{\pi}\delta(1-x)\delta(\mathbf{k}^2 - Q_0^2) + \bar{\alpha}_s \int \frac{\mathrm{d}^2\mathbf{q}}{\pi \mathbf{q}^2} \int_x^1 \frac{\mathrm{d}z}{z} \big[\mathscr{F}(x/z, \mathbf{k}+\mathbf{q}; Q_0) - \Theta(k-q)\mathscr{F}(x/z,\mathbf{k};Q_0) \big] . \tag{2.16}$$

The first term under the integral of eq. (2.16) represents real gluon emission, and the second one a new form of virtual corrections, typical of the small-x problem, and discussed at length in refs. [7,8]. It is apparent that there is no explicit form of $k_\perp$-ordering in eq. (2.16), the $\mathbf{q}$-integration being unrestricted, with $0 \leqslant \mathbf{q}^2 < \infty$. The role of the virtual term is precisely that of regulating the $\mathbf{q}^2 = 0$ singularity and of suppressing in part the *disordered* region $k_\perp \simeq |k_\perp + q_\perp| > |q_\perp|$, thus leading to the approximate $k_\perp$-ordering ($k_\perp > |k_\perp + q_\perp|$) which is a feature of the one-loop Altarelli–Parisi equation.

In order to resum small-x corrections, one has to solve eq. (2.16), and insert it into eq. (2.3). It is clear that such corrections will be transferred by the z-convolution and $k_\perp$-integration into the cross section $\sigma_{\gamma g}$, and they will appear perturbatively as powers of $\ln \rho$ both in the coefficient function (the one we are looking for) and in the anomalous dimension part.

The known [4–9] explicit solution of eq. (2.16) is found easier by the scale invariance of its kernel, and reveals some novel features of small-x physics, but also raises a few questions in comparison with the renormalization group approach.

Following, e.g. ref. [4], it is convenient to introduce the Mellin transform

$$\mathscr{F}_N(\mathbf{k}; Q_0^2) \equiv \int_0^1 \mathrm{d}x\, x^{N-1} \mathscr{F}(x, k; Q_0^2), \tag{2.17}$$

and to rewrite eq. (2.16) in N-moment space by using the change of variables $\mathbf{k}' = \mathbf{k} + \mathbf{q}$ and by performing the relevant azimuthal averaging, in the form

$$\begin{aligned} &\mathscr{F}_N(\mathbf{k}^2; Q_0^2) - \frac{1}{\pi}\delta(k^2 - Q_0^2) \\ &\quad \equiv \frac{\bar{\alpha}_s}{N} H \mathscr{F}_N(\mathbf{k}^2; Q_0^2) \\ &\quad = \frac{\bar{\alpha}_s}{N} \int_0^1 \frac{\mathrm{d}\lambda}{1-\lambda} \left[\mathscr{F}_N(\lambda \mathbf{k}^2; Q_0^2) + \frac{1}{\lambda} \mathscr{F}_N(\mathbf{k}^2/\lambda; Q_0^2) - 2\mathscr{F}_N(\mathbf{k}^2; Q_0^2) \right]. \end{aligned} \tag{2.18}$$

The kernel H in eq. (2.18) has power-like eigenfunctions of the form $(\mathbf{k}^2)^{\gamma-1}$ corresponding to the eigenvalues [5]

$$f(\gamma) = 2\psi(1) - \psi(\gamma) - \psi(1-\gamma), \tag{2.19}$$

given in terms of the Euler ψ-function (fig. 5). This set of eigenfunctions constitutes a proper continuum spectral family for $\gamma = 1/2 + i\sigma$, so that eq. (2.18) is

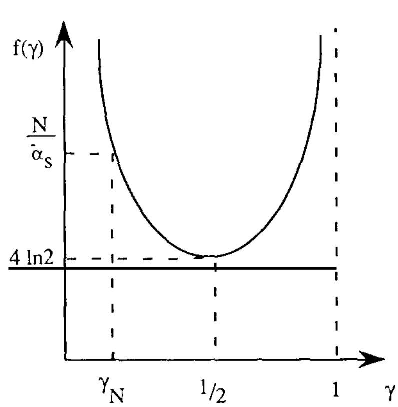

Fig. 5. Lipatov characteristic function $f(\gamma)$ for the gluon anomalous dimension.

diagonalized by a Fourier transform in the variable $\ln \mathbf{k}^2/Q_0^2$. The solution for $\mathscr{F}$, in N-moment space, is therefore

$$\mathscr{F}_N(\mathbf{k}; Q_0^2) = \frac{1}{\pi \mathbf{k}^2} \int_{\frac{1}{2}-i\infty}^{\frac{1}{2}+i\infty} \frac{\mathrm{d}\gamma}{2\pi i} \left(1 - \frac{\bar{\alpha}_s}{N} f(\gamma)\right)^{-1} \left(\frac{\mathbf{k}^2}{Q_0^2}\right)^{\gamma}. \tag{2.20}$$

A full discussion of eq. (2.20) is needed in order to understand the philosophy that will be followed in this paper and it will concern in order the consistency with renormalization group factorization, the Q_0 parameter and the running of α_s, which is being kept frozen in this section.

Note first that the integrand of eq. (2.20) shows pole singularities at

$$1 = \frac{\bar{\alpha}_s}{N} f(\gamma_N), \tag{2.21}$$

where $f(\gamma)$, given by eq. (2.19), has an infinity of poles both for $\gamma < 1/2$ ($\gamma = 0, -1, -2, \dots$) and for $\gamma > 1/2$ ($\gamma = 1, 2, \dots$). The left poles of f come from $\psi(\gamma)$ in (2.19) and originate from the region of ordered momenta $(\mathbf{k}+\mathbf{q})^2 < \mathbf{k}^2$ in eq. (2.16), while the right poles come from $\psi(1-\gamma)$ and originate from the disordered ones $(\mathbf{k}+\mathbf{q})^2 \geqslant \mathbf{k}^2$. The poles of $f(\gamma)$ nearest to $\gamma = 1/2$ are at $\gamma = 0$ (left) and at $\gamma = 1$ (right) and are shown in fig. 5.

In order to express the solution (2.20) as a sum of anomalous dimension contributions, one has to displace the γ-contour from $\mathrm{Re}\,\gamma = 1/2$ to pick up the poles defined by eq. (2.21). It is convenient to do it towards the left for $\mathbf{k}^2 > Q_0^2$. For sufficiently small values of $\bar{\alpha}_s/N < (4 \ln 2)^{-1}$ (*perturbative regime*), it appears from fig. 5 that a solution of (2.21) exists with $\gamma \ll 1$, which follow from the behaviour

$$f(\gamma) = \frac{1}{\gamma} + 2\zeta(3)\gamma^2 + \mathrm{O}(\gamma^4), \qquad (\gamma \ll 1), \tag{2.22}$$

and has the expansion mentioned in sect. 1

$$\gamma_N(\alpha_s) = \frac{\bar{\alpha}_s}{N} + 2\zeta(3)\left(\frac{\bar{\alpha}_s}{N}\right)^4 + \mathrm{O}\left(\left(\frac{\bar{\alpha}_s}{N}\right)^6\right), \qquad \zeta(3) \simeq 1.202, \tag{2.23}$$

ζ being the Riemann ζ-function. This solution, that will be called the perturbative branch of the anomalous dimension, is consistent [4] with known calculations up to two loops and gives a good representation of $\mathscr{F}_N$ for $\mathbf{k}^2 \gg Q_0^2$ in the perturbative regime

$$\mathscr{F}_N(\mathbf{k};Q_0^2)=\frac{1}{\pi\mathbf{k}^2}\left(\frac{\mathbf{k}^2}{Q_0^2}\right)^{\gamma_N}\left[-\frac{\bar{\alpha}_s}{N}f'(\gamma_N)\right]^{-1}\left[1+O\left(\frac{Q_0^2}{\mathbf{k}^2}\right)\right]. \tag{2.24}$$

In this regime, the full gluon structure function, integrated up to the scale $Q^2>Q_0^2$ is thus given by

$$\begin{aligned}G_N(Q^2/Q_0^2)&\equiv\int_0^{Q^2}\mathrm{d}^2\mathbf{k}\,\mathscr{F}_N(\mathbf{k};Q_0^2)\\&\simeq\left(\frac{Q^2}{Q_0^2}\right)^{\gamma_N}\left[-\frac{\bar{\alpha}_s}{N}\gamma_N f'(\gamma_N)\right]^{-1}.\end{aligned} \tag{2.25}$$

However, for larger values of $\bar{\alpha}_s/N$, γ_N increases quite fast, and for $\bar{\alpha}_s/N=(4\ln 2)^{-1}$ reaches the value $\gamma=1/2$ at which $f(\gamma)$ has a minimum. For still larger values of $\bar{\alpha}_s/N$ (larger than $(4\ln 2)^{-1}$), there are two complex conjugate branches of γ_N, coming from the pinching with the symmetrical solution of eq. (2.21) at $\gamma=1-\gamma_N$. The branch point value at $N=\bar{N}=4\bar{\alpha}_s\ln 2$ corresponds to a power increase with S of the structure function (*perturbative Pomeron*) and calls for unitarization corrections [9, 10].

All this is perhaps well known [4–10], but teaches us a few lessons in the present context. It is now clear, in fact, that the small-x equation (2.16) *is not* a generalized evolution equation in $k_\perp$. In particular, $\mathscr{F}_N(\mathbf{k};Q_0^2)$ *does not* vanish for $\mathbf{k}^2<Q_0^2$, because of the right poles in the γ-plane in eq. (2.20), and it *cannot* be described in terms of a single anomalous dimension in the full N-range.

As a consequence, the Q_0 parameter introduced here does not have the exact meaning of factorization scale between perturbative and non-perturbative physics. In the present context, for a realistic calculation of hadronic structure functions, one should rather provide a non-perturbative Q_0-*distribution* of the gluon in the hadron to be convoluted with $\mathscr{F}_N(\mathbf{k};Q_0^2)$. In other words, the small-x equation needs a $k_\perp$-dependent vertex both for the hard probe (where it is provided by the hard cross section $\hat{\sigma}$ treated in the present paper) and for the soft probe (where so far we only know integrated structure functions defined by renormalization group factorization properties).

Fortunately, in the perturbative regime $\bar{\alpha}_s/N\ll 1$ the situation simplifies, the factorized expression (2.24) holds, $k_\perp$-ordering is valid, Q_0 acquires the meaning of factorization scale with respect to soft physics and $\mathscr{F}_N(\mathbf{k};Q_0^2)$ can safely be multiplied by a non-perturbative structure function integrated up to Q_0. Thus Q_0 acts in this case as a lower cut-off on the transverse momentum $\mathbf{k}$ and the corresponding factorization scheme turns out to be equivalent to the $\overline{\mathrm{MS}}$ scheme in dimensional regularization [3]. But the perturbative regime is not self-contained because the expression of γ_N, if taken from (2.20), has a branch-point for $N = 4\bar{\alpha}_s \ln 2$, divides in two branches and calls for a not fully factorized expression at extreme energies.

A similar question arises for the introduction of a running coupling constant. Strictly speaking, the running coupling effects mix with subleading $\ln x$ contributions and can thus be neglected at the stage of LLA. Nevertheless, in the perturbative regime, where a single anomalous dimension dominates, it is still possible to introduce a running α_s by asking consistency with the renormalization group, as will be done in sect. 3. This method becomes ambiguous in the full energy (or N-moment) range, because of the contribution of other anomalous dimension branches. Modified small-x equations have been discussed [9, 10] but are not free, we believe, of the same intrinsic ambiguity.

To sum up, the consistency requirements of multi-Regge factorization (as embodied in the small-x equation (2.16)) with renormalization group factorization properties are not, as yet, fully understood at the structure function level. Nevertheless, it is quite possible to work out the consequences of the former on the latter, at the level of the hard probe, on the basis of eq. (2.3). We shall do that in sect. 3, exhibiting analytical results for the K-factors involved.

We conclude this section by noticing that the $k_\perp$-factorization theorem and the ensuing resummation effects have a straightforward generalization to the case of incoming quarks. For instance, the photoproduction cross section $\sigma_{\gamma q}$ is given by eq. (2.3) replacing the gluon structure function $\mathscr{F}$ with the quark structure function $\mathscr{F}^{(q)}$. This latter satisfies the Lipatov equation ($C_F = (N_c^2 - 1)/2N_c$)

$$\mathscr{F}^{(q)}(x, \mathbf{k}; Q_0^2) = \frac{C_F \alpha_s}{\pi^2 \mathbf{k}^2} \Theta(\mathbf{k}^2 - Q_0^2) + \bar{\alpha}_s \int \frac{d^2\mathbf{q}}{\pi \mathbf{q}^2} \int_x^1 \frac{dz}{z} \left[\mathscr{F}^{(q)}(x/z, \mathbf{k}+\mathbf{q}; Q_0^2) - \Theta(k-q) \mathscr{F}^{(q)}(x/z, \mathbf{k}; Q_0^2) \right], \tag{2.26}$$

whose solution in N-moment space reads

$$\mathscr{F}_N^{(q)}(\mathbf{k}; Q_0^2) = \frac{C_F \alpha_s}{\pi^2 N \mathbf{k}^2} \int_{\frac{1}{2}-i\infty}^{\frac{1}{2}+i\infty} \frac{d\gamma}{2\pi i \gamma} \left(1 - \frac{\bar{\alpha}_s}{N} f(\gamma)\right)^{-1} \left(\frac{\mathbf{k}^2}{Q_0^2}\right)^{\gamma}. \tag{2.27}$$

3. Resummation and energy dependence

The factorization formula (2.3) is a convolution in the ρ variable. Therefore, it is convenient to write it in N-moment space, by introducing the representation (2.20) of the gluon structure function. We obtain

$$4M^2\sigma_{\gamma g,N}\left(\frac{M^2}{Q_0^2}\right) = \int d^2\mathbf{k}\, \mathscr{F}_N(\mathbf{k};Q_0^2)\hat{\sigma}_N\left(\frac{\mathbf{k}^2}{M^2}\right)$$

$$= \int_{\frac{1}{2}-i\infty}^{\frac{1}{2}+i\infty} \frac{d\gamma}{2\pi i}\left(\frac{M^2}{Q_0^2}\right)^{\gamma}\left(1-\frac{\bar{\alpha}_s}{N}f(\gamma)\right)^{-1}\frac{1}{\gamma}h_N(\gamma), \quad (3.1)$$

where we have introduced the function $h(\gamma)$ which is a weighted $k_\perp$-average of the cross section $\hat{\sigma}$, defined by

$$\frac{1}{\gamma}h_N(\gamma) = \int_0^\infty \frac{d\mathbf{k}^2}{\mathbf{k}^2}\left(\frac{\mathbf{k}^2}{M^2}\right)^{\gamma}\hat{\sigma}_N\left(\frac{\mathbf{k}^2}{M^2}\right). \quad (3.2)$$

In order to analyze eqs. (3.1) and (3.2) in detail, we need the explicit form of the off-shell Born cross section. From the definition (2.15) we obtain the differential cross section

$$d\hat{\sigma}\left(\frac{\rho}{z},\xi,\frac{\mathbf{k}^2}{M^2}\right) = \frac{\rho}{z}A_2\left(\frac{\rho}{z},\xi,\frac{\mathbf{k}^2}{4M^2}\right)d\Phi \quad (3.3)$$

where we have introduced the angular variable

$$\xi = 4\tau(1-\tau), \qquad \tau = \frac{M^2-t}{zS} \quad (3.4)$$

and the phase space factor (appendix A)

$$d\Phi = \frac{1}{16\pi}\frac{d\xi}{\sqrt{1-\xi}}\Theta\left(\frac{z}{\rho}-\frac{1}{\xi}-\frac{\mathbf{k}^2}{4M^2}\right)\Theta(1-\xi)\Theta(\xi). \quad (3.5)$$

The spin averaged absorptive part A_2 is in turn obtained by a straightforward calculation (appendix C) of the abelian diagrams in fig. 1, and is given by a second-order polynomial in $k_\perp^2$ as follows

$$A_2\left(\rho,\xi,\frac{\mathbf{k}^2}{4M^2}\right) = 32\pi^2\alpha\alpha_s e_Q^2\frac{1}{\xi}\sum_{n=0}^{2}a_n(\rho,\xi)\left(\frac{\mathbf{k}^2}{4M^2}\right)^n,$$

$$a_0 = 1-\tfrac{1}{2}\xi+\rho-\frac{\rho^2}{\xi},$$

$$a_1 = \rho\left(3\xi-2-4\rho+\frac{2\rho}{\xi}\right),$$

$$a_2 = \rho^2(2-3\xi). \quad (3.6)$$

Finally, in the analysis of (3.1) we are mostly interested in the high-energy (small-N) behaviour of $\sigma_{\gamma g}$, whose Born term is uniformly small, due to the fermion exchange diagrams in fig. 1. For instance, from eq. (3.6), in the limit $\rho \to 0$ with $\rho k_\perp^2 = O(M^2)$ fixed, we have*

$$\hat{\sigma}(\rho, \mathbf{k}^2/M^2) \simeq 2\pi\alpha e_Q^2 \alpha_s \rho \ln\frac{1}{\rho}\Theta\left(\frac{1-\rho}{\rho} - \frac{\mathbf{k}^2}{4M^2}\right) \times \left[\left(1 - \frac{\rho\mathbf{k}^2}{4M^2}\right)^2 + \left(\frac{\rho\mathbf{k}^2}{4M^2}\right)^2\right]. \tag{3.7}$$

It follows that both $\hat{\sigma}_N(k_\perp^2/M^2)$ and $h_N(\gamma)$ are weakly N-dependent, so that, in the small-ρ regime $N \ll \gamma$, we can set $N = 0$ in eq. (3.2)

$$h_N(\gamma) = h(\gamma)(1 + O(N)), \qquad (N \ll \gamma). \tag{3.8}$$

The complete calculation of $h(\gamma)$ then gives (appendix C)

$$h(\gamma) = \frac{4\pi}{3}\alpha\alpha_s e_Q^2 \frac{7-5\gamma}{3-2\gamma} B(1-\gamma, 1-\gamma) B(1+\gamma, 1-\gamma), \tag{3.9}$$

where B is Euler's beta function.

The expression (3.9) for $h(\gamma)$ is analytic in the region $0 \leqslant \mathrm{Re}\,\gamma < 1$ which is needed in eq. (3.1). The finite value of $h(0)$ corresponds to a pole contribution to eq. (3.2) from the small $k_\perp$ region, and is given by the $N = 0$ moment of the on-shell Born term of eq. (1.1)

$$h(0) \equiv h_{\mathrm{Born}}(\gamma) = 4M^2 \int_0^1 \frac{d\rho}{\rho} \sigma_{\gamma g, \mathrm{Born}}(\rho) = \tfrac{28}{9}\pi\alpha\alpha_s e_Q^2. \tag{3.10}$$

A similar $\gamma = 0$ pole occurs in eq. (3.2) for any value of N, with residue $h_N(0) = \hat{\sigma}_N(0)$, thus showing that eq. (3.1) is consistent with the usual renormalization group factorization in the small γ limit. Note however that $h(\gamma)$ quickly increases as $\gamma \to 1$ (fig. 6) and has a double pole singularity at $\gamma = 1$. This pole stems from the small ρ, large $k_\perp$ behaviour of eq. (3.7), which implies

$$\hat{\sigma}_N(\mathbf{k}^2/M^2) \simeq \frac{16\pi}{3}\alpha e_Q^2 \alpha_s \frac{M^2}{\mathbf{k}^2} \ln\frac{\mathbf{k}^2}{M^2}, \tag{3.11}$$

* Notice the amusing fact that the coefficient of $\rho \ln 1/\rho$ in eq. (3.7) is just the Altarelli–Parisi splitting function for $g \to q\bar{q}$ in the momentum fraction variable $\bar{z} = \rho\mathbf{k}^2/4M^2$. This is due to the dominance of the collinear singularity $(k - p_4)^2 = M^2((k - p_3)^2 = M^2)$ in this region.

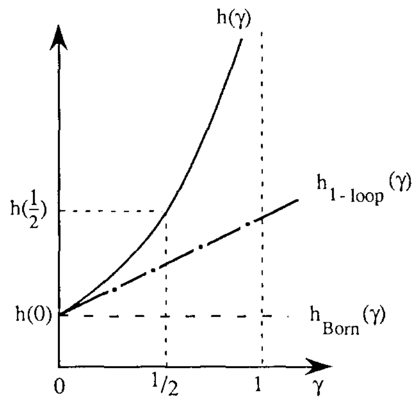

Fig. 6. Resummed (h), 1-loop ($h_{1\text{-loop}}$) and Born (h_{Born}) hard cross section functions for photoproduction.

where the logarithmic enhancement is related to the t-channel collinear singularity for $M^2 \to 0$.

Let us now discuss the result (3.1) in various regimes on the basis of the explicit expression (3.9) of $h(\gamma)$. The perturbative regime is defined by $\bar{\alpha}_s/N \ll 1$ in moment space, or by $\bar{\alpha}_s \ln 1/\rho \ll \ln M^2/Q_0^2$ in energy space. In this region, the γ-integral is done by going to the pole of eq. (2.21) which implicitly defines the perturbative branch of the anomalous dimension $\gamma_N \equiv \gamma(\bar{\alpha}_s/N)$ in eq. (2.23). We thus obtain

$$4M^2\sigma_{\gamma g,N}(M^2/Q_0^2) = G_N(M^2/Q_0^2)h_N(\gamma_N), \qquad (3.12)$$

where we have introduced the gluon structure function

$$G_N(M^2/Q_0^2) = \int_0^{M^2} \mathrm{d}^2\mathbf{k}\, \mathcal{F}_N(\mathbf{k}; Q_0^2)$$

$$= \left(\frac{M^2}{Q_0^2}\right)^{\gamma_N}\left[-\frac{\bar{\alpha}_s}{N}\gamma_N f'(\gamma_N)\right]^{-1}. \qquad (3.13)$$

A result similar to eq. (3.12) has been announced by other authors [14].

The expression (3.12) is consistent with the standard QCD factorization theorem [15] in which $h_N(\gamma_N(\alpha_s))$ represents the resummed expression of the coefficient function we were looking for. The resummation effect is incorporated in eq. (3.12) through the (α_s/N) dependence of γ_N known from eq. (2.23) and the γ-dependence of $h_N(\gamma) \simeq h(\gamma)$ known from eq. (3.9).

In other words, the usual RG factorization property is recovered in this perturbative regime, with an improved coefficient function. Furthermore, due to the dominance of the anomalous dimension γ_N, running coupling constant effects can be introduced by using RG evolution equations, i.e. by the replacement

$$\left(\frac{M^2}{Q_0^2}\right)^{\gamma_N} \to \exp\left[\int_{Q_0^2}^{M^2} \frac{dk^2}{k^2} \gamma_N\big(\alpha_s(k^2)\big)\right]. \tag{3.14}$$

As far as the coefficient function $h_N(\gamma_N(\alpha_s))$ is concerned, the argument of α_s is fixed at M^2 because the running of the coupling constant gives rise to subleading logarithmic contributions. In fact, due to the suppression factor $M^2/\mathbf{k}^2$ in the hard cross section (3.11), the introduction of a running coupling $\alpha_s(\mathbf{k}^2) = \alpha_s(M^2) \times(1 - b\alpha_s(M^2)\ln M^2/\mathbf{k}^2 + \dots)$ in eq. (3.2) for $\mathbf{k}^2 \gg M^2$ leads to perturbative corrections (i.e. of order $\alpha_s(M^2)$ without the singular coefficient N^{-1}) for $h_N(\gamma)$ in the physical range $0 \leqslant \gamma < 1/2$.

Finally, the perturbative QCD calculations for $N < \gamma_N$, are reproduced by power expansion in α_s of eq. (3.12). For instance, at one-loop level we obtain from eq. (3.9)

$$h_{1\text{-loop}}(\gamma) = h(0)\big(1 + \tfrac{41}{21}\gamma\big), \tag{3.15}$$

in agreement with eqs. (1.2) and (1.5).

If $\bar{\alpha}_s/N$ is too large ($N/\bar{\alpha}_s < \mathrm{f}(\gamma_{\min} = 1/2) = 4\ln 2$) or ρ is too small ($\bar{\alpha}_s \ln 1/\rho > \ln M^2/Q_0^2$) the perturbative anomalous dimension (2.23) divides in two branches, the solutions of eq. (2.21) becoming complex conjugate. In this "extreme energy" regime, the result (3.1) in moment space requires at least two anomalous dimension contributions. Thus, as discussed in sect. 2, it is not strictly consistent with a simple renormalization group factorization property. Therefore, it is more convenient to discuss directly the energy dependence of the cross section, which is obtained from eq. (3.1) by inverse Mellin transform. By performing the N-integration first at the pole in eq. (2.21), we obtain, for $S \gg 4M^2$,

$$4M^2\sigma_{\gamma g}\left(\rho, \frac{M^2}{Q_0^2}\right) \simeq \int_{\frac{1}{2}-i\infty}^{\frac{1}{2}+i\infty} \frac{d\gamma}{2\pi i} \frac{\bar{\alpha}_s f(\gamma)}{\gamma} h(\gamma)\left(\frac{M^2}{Q_0^2}\right)^{\gamma}\left(\frac{S}{4M^2}\right)^{\bar{\alpha}_s f(\gamma)}. \tag{3.16}$$

The γ-integral is then evaluated by saddle point method. The stationary phase condition is

$$\bar{\alpha}_s L f'(\bar{\gamma}) + l = 0, \qquad \big(l = \ln M^2/Q_0^2,\ L = \ln 1/\rho\big), \tag{3.17}$$

and yields

$$4M^2\sigma_{\gamma g}(\rho, M^2/Q_0^2) = G(\rho, M^2/Q_0^2)h(\bar{\gamma}), \tag{3.18}$$

where $h(\bar{\gamma})$ is the hard cross section factor and the gluon structure function is

$$G(\rho, M^2/Q_0^2) \simeq \left(\frac{M^2}{Q_0^2}\right)^{\bar{\gamma}} \left(\frac{S}{4M^2}\right)^{\bar{\alpha}_s f(\bar{\gamma})} \frac{\bar{\alpha}_s f(\bar{\gamma})}{\bar{\gamma}\sqrt{2\pi\bar{\alpha}_s L f''(\bar{\gamma})}}. \tag{3.19}$$

At intermediate energies, such that $\bar{\alpha}_s L \ll l$, the stationary point is $\bar{\gamma} \simeq (\bar{\alpha}_s L/l)^{1/2}$, and we obtain

$$G(\rho, M^2/Q_0^2) \simeq (1/\sqrt{4\pi})(\bar{\alpha}_s l)^{1/4} L^{-3/4} \exp\left(2\sqrt{\bar{\alpha}_s L l}\right), \tag{3.20}$$

$$h(\bar{\gamma}) = \left[1 + \tfrac{41}{21}\sqrt{\bar{\alpha}_s L/l} + \mathrm{O}(\bar{\alpha}_s L/l)\right]. \tag{3.21}$$

The gluon structure function (3.20) has the exponential behaviour [9] obtained by solving the Altarelli–Parisi equation, or the Lipatov equation in the one-loop regime ($f(\gamma) \simeq 1/\gamma$). $h(\gamma)$ takes a perturbative form so that the resummed result (3.21) gives small corrections with respect to calculations at fixed order in α_s.

In the opposite regime of extreme energies ($\bar{\alpha}_s L \gg l$), the saddle point drifts towards the minimum of $f(\gamma)$ at $\gamma = 1/2$, so that the gluon structure function has a power dependence on S as given by the perturbative QCD pomeron [9]

$$G(\rho, M^2/Q_0^2) \simeq \sqrt{\frac{M^2}{Q_0^2}} \frac{8\bar{\alpha}_s \ln 2}{[56\pi\zeta(3)\bar{\alpha}_s L]^{1/2}} \left(\frac{S}{4M^2}\right)^{4\bar{\alpha}_s \ln 2} \tag{3.22}$$

and the total cross section is

$$4M^2\sigma_{\gamma g}(\rho, M^2/Q_0^2) = G(\rho, M^2/Q_0^2)h(1/2), \tag{3.23}$$

where, by eq. (3.9),

$$h(1/2) = \tfrac{3}{2}\pi^3\alpha\alpha_s e_Q^2. \tag{3.24}$$

We do not discuss here the introduction of a running coupling constant in this extreme energy regime, due to the ambiguities connected with it, and discussed in sect. 2. We stress however the point that the asymptotic factorized result (3.23) is only dependent on the fact that the anomalous dimension saturates at $\gamma = 1/2$, and not on the details of the structure function calculations.

We are now in a position to discuss the size of the large $(\alpha_s \ln \rho)^n$ corrections resummed in the asymptotic formulas (3.23) and (3.24). The value $h(1/2)$ on the right-hand side of eq. (3.23) is the result of the resummation for the hard cross section contributions. In lowest order perturbative calculations it is replaced by $h_{\mathrm{Born}}(1/2)$ or $h_{\mathrm{1\text{-}loop}}(1/2)$ with the Born and 1-loop hard cross section function respectively given in eqs. (3.10) and (3.15). We can see that the resummed value (3.24) is approximately a *factor of five* larger than the Born cross section factor

$$\frac{h(1/2)}{h_{\mathrm{Born}}(1/2)} = \frac{27}{56}\pi^2 \tag{3.25}$$

and still a *factor of* 2.5 larger than the corresponding 1-loop value

$$\frac{h(1/2)}{h_{\mathrm{1\text{-}loop}}(1/2)} = \frac{81}{332}\pi^2, \tag{3.26}$$

leading to a corresponding increase in the photoproduction total cross section (3.23) at very high energies.

Obviously, the result (3.23) is valid only in the asymptotic regime. Nevertheless a value of the resummed cross section larger than that predicted by lowest-order calculations is expected even for lower energies. This trend can be argued by comparing the resummed, 1-loop and Born cross section functions h for any values of γ (fig. 6). As discussed before, the steep behaviour of $h(\gamma)$ in eq. (3.9) is due to the physical shape (3.11) of $\hat{\sigma}_N(\mathbf{k}^2/M^2)$, which does not provide a sharp cut-off for large $k_\perp$ values. Therefore features similar to those illustrated so far are expected for any production cross section involving one initial state gluon.

One more point we want to emphasize is that the summed asymptotic value in eq. (3.24) is just a finite constant, showing no trace of the leading powers of $\ln 1/\rho$ it originated from. This is due to the structure of the perturbative series for large S. As we can see from the leading logarithmic result in eq. (3.12), one can have at most one power of $\ln \rho$ for each power of α_s. This result follows from the smoothness of $h(\gamma)$ for $0 \leqslant \gamma < 1$, which in turn derives from the fact that $\hat{\sigma}(\rho, \mathbf{k}^2/M^2)$ in eq. (3.7) is *uniformly* small, of order ρ, even close to the phase space boundary of large $k_\perp = \mathrm{O}(\sqrt{S}\,)$. In contrast, a point-like probe as given by the current $J = F^a_{\mu\nu}F^{\mu\nu a}$ would yield

$$\hat{\sigma}_{\mathrm{point}}(\rho) = \frac{1}{\rho}\delta\left(\frac{1}{\rho} - 1 - \frac{k_\perp^2}{Q^2}\right),$$

$$\hat{\sigma}_{\mathrm{point},N} = \left(1 + \frac{k_\perp^2}{Q^2}\right)^{-N} \xrightarrow{N\to 0} 1, \tag{3.27}$$

thus causing an additional singularity of eq. (3.2) at $\gamma = N$, and eventually *double*-log terms ($\sim \alpha_s/N^2$) in the coefficient function.

The above remarks illustrate the fact that the $Q\bar{Q}$ system is a non-local probe of the gluon $k_\perp$ dependence, which cuts off the $k_\perp$-integration around $k_\perp \simeq M \ll \sqrt{S}$. For a local probe large values of $k_\perp = O(\sqrt{S})$ are allowed, yielding a much stronger singularity of the coefficient of type α_s/N^2 (as for time-like jet evolution [4]). It is rather peculiar that no such local probe seems available in nature for gluons. Indeed, even produced jets, corresponding to emitted gluons, are screened by strong virtual corrections [7, 8], which do not allow values of $k_\perp$ larger than the jet mass. This fact seems to be yet another manifestation of colour confinement.

4. The lepto-production case

Let us investigate $Q\bar{Q}$ production in the more general cases of lepton- and hadron-initiated processes. We start considering the $Q\bar{Q}$ lepto-production process off external gluons and via off-shell photons (fig. 7), corresponding to the sub-process

$$\gamma^*(q) + g(k_2) \to \bar{Q}(p_3) + Q(p_4) + X, \tag{4.1}$$

which turns out to dominate c and b quark production in the TeV region [16]. The lepton differential cross section can be written as

$$d\sigma^{(e)} = \frac{\alpha}{\pi}\frac{dQ^2}{Q^2}\frac{dy}{y}\Theta\left(Q^2 - \frac{y^2m^2}{1-y}\right) \times\left[(1-y)\sigma_2\left(\frac{\rho}{y}, \frac{Q^2}{M^2}; \frac{M^2}{Q_0^2}\right) + \tfrac{1}{2}y^2\sigma_1\left(\frac{\rho}{y}, \frac{Q^2}{M^2}; \frac{M^2}{Q_0^2}\right)\right], \tag{4.2}$$

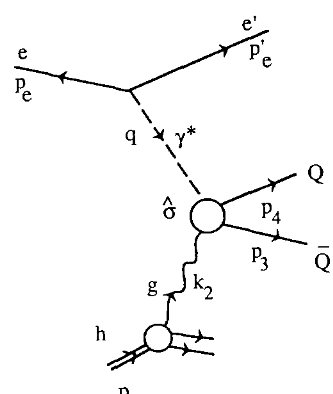

Fig. 7. The neutral current γg contribution to heavy flavour lepto-production.

where m is the mass of the charged lepton, σ_1 and σ_2 are related, in the $M \to 0$ limit, to the customary structure functions F_1 and F_2 for deep inelastic scattering (DIS) by the relations

$$\sigma_1 = \frac{4\pi^2\alpha}{Q^2} 2x_B F_1, \qquad \sigma_2 = \frac{4\pi^2\alpha}{Q^2} F_2, \qquad (M^2 = 0), \tag{4.3}$$

and Q^2, y, ρ and the Bjorken variable x_B are defined by (appendix A)

$$Q^2 = -q^2, \qquad S = 2p_1 \cdot p_2,$$

$$y = \frac{p_2 \cdot q}{p_2 \cdot p_1}, \qquad \rho = \frac{4M^2}{S}, \qquad x_B = \frac{Q^2}{2p_2 \cdot q} = \frac{Q^2\rho}{4M^2 y}. \tag{4.4}$$

4.1. FACTORIZATION FORMULA

In the small-x ($x = x_B, \rho$) limit, we propose again the $k_\perp$-dependent factorization structure of fig. 2b corresponding to the high-energy Regge exchange of a single gluon $g(k_2)$, as in fig. 4a. Since small values of x can be obtained, in the $\rho \to 0$ limit, for any fixed value of Q^2/M^2 and y, factorization formulae hold for each one of the structure functions F_i, or cross sections σ_i.

More precisely, we write

$$4M^2\sigma_i\left(\frac{\rho}{y}, \frac{Q^2}{M^2}; \frac{M^2}{Q_0^2}\right) = \int d^2\mathbf{k}_2 \int_0^1 \frac{dz_2}{z_2} \hat{\sigma}_i\left(\frac{\rho}{yz_2}, \frac{\mathbf{q}}{M}, \frac{\mathbf{k}_2}{M}\right) \mathscr{F}(z_2, \mathbf{k}_2; Q_0^2), \tag{4.5}$$

where the $\hat{\sigma}_i$'s are defined from the high-energy limit of the abelian diagrams in fig. 8, with an incoming off-shell photon $\gamma^*(q)$. In other words, $\hat{\sigma}_1$ and $\hat{\sigma}_2$ are obtained by coupling the initial gluon $g(k_2)$ to external partons by eikonal vertices and projecting out the two structure functions (4.3) at the photon vertex as in eq. (4.2). The hard cross section $\hat{\sigma}_2$ is evaluated in appendix C.

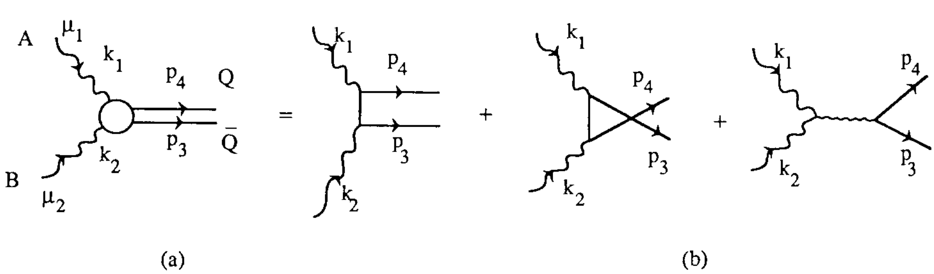

Fig. 8. Born diagrams with off-shell incoming lines for lepto-production and hadro-production.

The small-y limit in eq. (4.2) is dominated by the cross section σ_2, which also measures the sum of the transverse and longitudinal cross sections ($\sigma_2 = \sigma_T + \sigma_L$, up to a flux factor). Furthermore, both σ_1 and σ_2 reduce on-shell to the photo-production cross section

$$\sigma_1(\rho, 0; M^2/Q_0^2) = \sigma_2(\rho, 0; M^2/Q_0^2) = \sigma_{\gamma g}(\rho, M^2/Q_0^2). \qquad (4.6)$$

These remarks are useful for the evaluation of the *total* electro-production cross section in which the presence of two scales, Q^2 and M^2, plays an important role. This is because at high energies $S \gg M^2$ ($\rho \to 0$) the cross section is dominated by the small-y region in eq. (4.2), so that

$$\sigma^{(e)}(\rho, M^2/Q_0^2; M^2/m^2) \simeq \frac{\alpha}{\pi}\int_0^1 \frac{dy}{y}\int_{y^2m^2}^{\infty}\frac{dQ^2}{Q^2}\sigma_2(\rho/y, Q^2/M^2; M^2/Q_0^2). \quad (4.7)$$

This expression is in turn dominated [12] by the small Q^2 region $M^2 \gg Q^2 > y^2m^2$ in which σ_2 reduces essentially to the photoproduction cross section σ, as in eq. (4.6). Finally one has the high-energy relation

$$\sigma^{(e)}(\rho, M^2/Q_0^2; M^2/m^2) \simeq \frac{\alpha}{\pi}\int_0^1 \frac{dy}{y}\ln\frac{M^2}{y^2m^2}\sigma_{\gamma g}(\rho/y, M^2/Q_0^2). \qquad (4.8)$$

The important point is that, due to the large heavy flavour mass, implying that $\alpha_s(M^2) \ll 1$, the expressions (4.7) and (4.8) are still perturbative, and therefore they can be evaluated by using either the factorization formula (3.1) or its generalization (4.5).

If, on the other hand, Q^2 and M^2 are of the same order, the distribution (4.2) notably differs from the photo-production limit and the off-shell effects are to be evaluated on the basis of eq. (4.5). Since $M^2 \gg \Lambda^2$ throughout our paper, we find it convenient to use again ρ-moments (instead of x_B-moments, typical of the $M \to 0$ limit) by then studying their Q^2/M^2 dependence. To this purpose we parametrize the off-shell dependence on both Q^2 and k_2^2 in the r.h.s. of eq. (4.5) by anomalous dimension variables γ_1 and γ_2 as follows

$$4M^2\sigma_{i,N}\left(\frac{Q^2}{M^2}, \frac{M^2}{Q_0^2}\right) = \int_{\frac{1}{2}-i\infty}^{\frac{1}{2}+i\infty}\frac{d\gamma_1}{2\pi i}\left(\frac{M^2}{Q^2}\right)^{\gamma_1}\int_{\frac{1}{2}-i\infty}^{\frac{1}{2}+i\infty}\frac{d\gamma_2}{2\pi i}\left(\frac{M^2}{Q_0^2}\right)^{\gamma_2}$$

$$\times\left[1 - \frac{\bar{\alpha}_s}{N}f(\gamma_2)\right]^{-1}\frac{1}{\gamma_1\gamma_2}h_N^{(i)}(\gamma_1, \gamma_2), \qquad (4.9)$$

where we have used the representation (2.20) of $\mathscr{F}_N(\mathbf{k}_2)$ and we have defined the double $k_\perp$-transform

$$\frac{1}{\gamma_1\gamma_2}h_N^{(i)}(\gamma_1,\gamma_2)=\int\frac{\mathrm{d}^2\mathbf{k}_1}{\pi\mathbf{k}_1^2}\left(\frac{\mathbf{k}_1^2}{M^2}\right)^{\gamma_1}\int\frac{\mathrm{d}^2\mathbf{k}_2}{\pi k_2^2}\left(\frac{\mathbf{k}_2^2}{M^2}\right)^{\gamma_2}\times\int_0^1\frac{\mathrm{d}\rho}{\rho}\rho^N\hat{\sigma}_i\left(\rho,\frac{\mathbf{k}_1}{M},\frac{\mathbf{k}_2}{M}\right). \tag{4.10}$$

Notice that, since $\hat{\sigma}_i(\rho)=\mathrm{O}(\rho\ln 1/\rho)$ as discussed before, $\hat{\sigma}_{i,N}$ and thus $h_N^{(i)}$ are weakly N-dependent for $N \ll \gamma_i$.

4.2. RESUMMATION IN THE PERTURBATIVE REGIME

In the perturbative regime $\bar{\alpha}_s/N \ll 1$, we can evaluate the γ_2 integral in the r.h.s. of eq. (4.9) by going to the pole (2.21) as for photo-production. By introducing the gluon structure function (3.13), we obtain the resummed factorization formula

$$4M^2\sigma_{i,N}(Q^2/M^2;M^2/Q_0^2)=G_N(M^2/Q_0^2)\int_{\frac{1}{2}-i\infty}^{\frac{1}{2}+i\infty}\frac{\mathrm{d}\gamma}{2\pi i\gamma}\left(\frac{M^2}{Q^2}\right)^{\gamma}h_N^{(i)}(\gamma,\gamma_N), \tag{4.11}$$

where $\gamma_N=\gamma_N(\bar{\alpha}_s/N)$ is the perturbative branch of the anomalous dimension defined by eq. (2.21).

Eq. (4.11) is to be compared with eq. (3.12). The resummation effects, including the Q^2/M^2 dependence, are now embodied in the functions $h_N^{(i)}(\gamma_1,\gamma_2)$ which, according to eq. (4.10), can be computed from the abelian diagrams in fig. 8 with two off-shell legs. The complete calculation is done in appendix C for $N=0$ and $i=2$ by recasting the $N=0$ moment of $\hat{\sigma}_2(\rho,\mathbf{k}_1/M,\mathbf{k}_2/M)$ in the following form

$$\begin{aligned}&\int_0^1\frac{\mathrm{d}\rho}{\rho}\hat{\sigma}_2(\rho,\mathbf{k}_1^2/M^2,\mathbf{k}_2^2/M^2)\\&\quad=\pi\alpha\alpha_s e_Q^2\int_0^1\frac{\mathrm{d}\xi_1}{\sqrt{1-\xi_1}}\int_0^1\frac{\mathrm{d}\xi_2}{\sqrt{1-\xi_2}}\frac{1}{1+\xi_1x_1+\xi_2x_2}\\&\qquad\times\left[1-\frac{\xi_1\xi_2(1+x_1+x_2)}{2(1+\xi_1x_1+\xi_2x_2)}-\frac{2x_1x_2\xi_1(1-\xi_1)\xi_2(1-\xi_2)}{(1+\xi_1x_1+\xi_2x_2)^2}\right],\\&\qquad\qquad(x_i\equiv\mathbf{k}_i^2/4M^2).\end{aligned} \tag{4.12}$$

Here $\hat{\sigma}_2(\rho, \mathbf{k}_1^2/M^2, \mathbf{k}_2^2/M^2)$ is obtained by averaging $\hat{\sigma}_2(\rho, \mathbf{k}_1/M, \mathbf{k}_2/M)$ over the azimuthal angle between $\mathbf{k}_1$ and $\mathbf{k}_2$.

From this representation and from the definition (4.10) we obtain the result (appendix C)

$$h_{N=0}^{(2)}(\gamma_1, \gamma_2) \equiv h(\gamma_1, \gamma_2) = \tfrac{1}{4}\pi^2 \alpha\alpha_s e_Q^2 g(\gamma_1, \gamma_2), \tag{4.13}$$

$$g(\gamma_1, \gamma_2) = [7 - 5(\gamma_1 + \gamma_2) + 3\gamma_1\gamma_2] 4^{\gamma_1+\gamma_2}$$
$$\times \frac{\Gamma(1+\gamma_1)\Gamma(1-\gamma_1)\Gamma(1+\gamma_2)\Gamma(1-\gamma_2)}{\Gamma(5/2-\gamma_1)\Gamma(5/2-\gamma_2)} \Gamma(1-\gamma_1-\gamma_2). \tag{4.14}$$

It is easy to see that, in the limit $\gamma_1 \to 0$, $h^{(2)}(\gamma_1, \gamma_2)$ reduces to the function $h(\gamma)$ of the photo-production case, i.e.

$$h^{(2)}(0, \gamma) = h(\gamma) = h^{(2)}(\gamma, 0). \tag{4.15}$$

This ensures that $\sigma_2 = \sigma_T + \sigma_L$ reduces, in the on-shell limit $Q^2 = 0$, to the photo-production cross section. In fact, for $Q^2 \ll M^2$, the γ-contour in eq. (4.11) can be closed to the left of the $\gamma = 0$ pole, thus yielding, by eq. (4.15), the same expression as in eq. (3.12).

Notice that $h^{(2)}(\gamma_1, \gamma_2)$ is now analytic for $0 \leqslant \mathrm{Re}(\gamma_1 + \gamma_2) < 1$. In this case the double pole of $h(\gamma)$ at $\gamma = 1$ is split into two simple poles of $h^{(2)}$ at $\gamma_1 + \gamma_2 = 1$ and at $\gamma_2 = 1$ (or $\gamma_1 = 1$). This is because from eq. (4.12), in the region $\mathbf{k}_2^2 \gg \mathbf{k}_1^2 \gg M^2$ with $\rho\mathbf{k}_2^2 = \mathrm{O}(\mathrm{M}^2)$ fixed, one has the asymptotic behaviour

$$\hat{\sigma}_2(\rho, k_1/M, k_2/M) \simeq 2\pi\alpha e_Q^2 \alpha_s \rho \ln\frac{\mathbf{k}_2^2}{\mathbf{k}_1^2} \Theta\left(\frac{1}{\rho} - \frac{\mathbf{k}_2^2}{4M^2}\right)$$
$$\times \left[\left(1 - \frac{\rho\mathbf{k}_2^2}{4M^2}\right)^2 + \left(\frac{\rho\mathbf{k}_2^2}{4M^2}\right)^2\right], \qquad (\mathbf{k}_2^2 \gg \mathbf{k}_1^2 \gg M^2), \tag{4.16}$$

implying that $\hat{\sigma}_2$ is uniformly of order ρ and $\mathbf{k}_1^2$ acts as a lower cut-off of the collinear logarithm in place of M^2 in eq. (3.7). From (4.10) and (4.16) it follows that, for $N = 0$, $h^{(2)}$ has a simple pole at $\gamma_1 + \gamma_2 = 1$ as shown in eqs. (4.13) and (4.14). Obviously the residue of such a pole cannot be computed by the approximation (4.16) because also the region $\mathbf{k}_2^2 \simeq \mathbf{k}_1^2 \gg M^2$ contributes.

Finally we point out that the N dependence of $h_N^{(2)}$ cannot be neglected if γ_1 and γ_2 are so large that $\gamma_1 + \gamma_2$ approaches 1. As a matter of fact, it appears from eq. (4.16) that, for large $k_\perp$'s, i.e. $\mathbf{k}_2^2 \gg \mathbf{k}_1^2 \gg M^2$, the ρ phase space is restricted by

$\rho < 4M^2/\mathbf{k}_2^2$. Therefore, for $N \neq 0$, eq. (4.10) shows a large $k_\perp$ pole of h_N at $\gamma_1 + \gamma_2 = 1 + N$ and not at $\gamma_1 + \gamma_2 = 1$. We shall see that this displacement plays some role in understanding the Q^2 dependence for $Q^2 \gg M^2$.

The above properties of $h^{(2)}$ are useful to compare eqs. (4.11) and (3.12). The ratio

$$K_N^{(2)}(Q^2/M^2) = \frac{\sigma_{2,N}(Q^2/M^2, M^2/Q_0^2)}{\sigma_{\gamma g,N}(M^2/Q_0^2)} = \frac{1}{h_N(\gamma_N)} \int_{\frac{1}{2}-i\infty}^{\frac{1}{2}+i\infty} \frac{d\gamma}{2\pi i\gamma} \left(\frac{M^2}{Q^2}\right)^{\gamma} h_N^{(2)}(\gamma, \gamma_N) \tag{4.17}$$

does not contain the structure function factor, and is therefore a check of the $k_\perp$-dependent factorization formula, or in other words an absolute (i.e. structure function independent) prediction of perturbative QCD.

The r.h.s. of eq. (4.17) is explicitly evaluated in appendix C on the basis of eq. (4.13) and gives the result

$$\begin{aligned} K_N^{(2)}\left(\frac{Q^2}{M^2}\right) = \left(1 + \frac{Q^2}{4M^2}\right)^{-N} \frac{3}{(7-5\gamma_N)(1+2\gamma_N)} \Bigg\{ \Bigg[2(1+\gamma_N)\frac{M^2}{Q^2} \\ + \left(1 + \frac{Q^2}{4M^2}\right)^{\gamma_N - 1} \left(2 + 3\gamma_N - 3\gamma_N^2 - 2(1+\gamma_N)\frac{M^2}{Q^2}\right) \\ \times F\left(1-\gamma_N, \tfrac{1}{2}; \tfrac{3}{2}; \frac{Q^2}{Q^2 + 4M^2}\right)\Bigg]\Bigg\}, \end{aligned} \tag{4.18}$$

where $F(a, b; c; x)$ is the hypergeometric function and the factor $(1 + Q^2/4M^2)^{-N}$ qualitatively takes into account the N dependence of $h_N^{(2)}$ for $Q^2 \gg M^2$, as discussed before.

Starting from $K_N^{(2)} = 1$ for $Q^2 \ll M^2$, this ratio decreases with increasing Q^2, reaching for $Q^2 \gg M^2$ the asymptotic form

$$K_N^{(2)}\left(\frac{Q^2}{M^2}\right) \simeq \left(\frac{4M^2}{Q^2}\right)^{1+N} \left[\left(\frac{Q^2}{4M^2}\right)^{\gamma_N} - 1\right] \frac{3}{7\gamma_N}, \qquad (Q^2 \gg M^2), \tag{4.19}$$

valid in the regime $N \ll \gamma_N \simeq \bar{\alpha}_s/N \ll 1$. The power dependence in eq. (4.19) exhibits the change of scale $M^2 \to Q^2$, expected in the $M^2 \ll Q^2$ limit, and can be interpreted as coming from the poles $\gamma_1 = 1 - \gamma_N + N$ and $\gamma_1 = 1 + N$ in the expression of $h_N^{(2)}$.

A simple application of eqs. (4.11) and (4.17) is the analytic evaluation of the perturbative contributions to the lepto-production cross section.

We start noticing that the off-shell Born cross section computed in appendix C has the explicit form

$$4M^2\sigma_{2,\mathrm{Born}}(\rho, Q^2/M^2) = \hat{\sigma}_2(\rho, Q^2/M^2, \mathbf{k}_2^2/M^2 = 0) = 2\pi\alpha e_Q^2 \alpha_s \Theta\left(\frac{1}{\rho} - 1 - \frac{Q^2}{4M^2}\right)$$
$$\times \rho\beta' \Bigg\{ \left[\left(1 + \rho - \tfrac{1}{2}\rho^2\right)\mathscr{L}(\beta') - 1 - \rho \right] + \left[8 + \rho - (2 + 3\rho) \right.$$
$$\left. \times \mathscr{L}(\beta') \right] \frac{\rho Q^2}{4M^2} + \left[-8 + 2\mathscr{L}(\beta') \right] \left(\frac{\rho Q^2}{4M^2} \right)^2 \Bigg\}, \tag{4.20}$$

where

$$\beta' = \sqrt{1 - \rho\left(1 - \frac{\rho Q^2}{4M^2}\right)^{-1}}, \tag{4.21}$$

and $\mathscr{L}(\beta)$ is the bremsstrahlung function in eq. (1.4). The result in eq. (4.20) agrees with previous calculations [17].

The perturbative corrections to σ_2 are found by expanding (4.11) in powers of α_s, i.e. the function $h(\gamma_N)K_N^{(2)}(Q^2/M^2)$ in powers of γ_N. By eq. (4.18) we find at lowest order

$$h(\gamma)K_N^{(2)}(Q^2/M^2) = h(0)\frac{3}{7}\Bigg\{ \left[\frac{2M^2}{Q^2} + \left(1 - \frac{M^2}{Q^2}\right) J\left(\frac{Q^2}{4M^2}\right) \right]$$
$$+ \gamma \left[\frac{10M^2}{3Q^2} + \left(\frac{13}{6} - \frac{5M^2}{3Q^2} \right) J\left(\frac{Q^2}{4M^2}\right) + \left(1 - \frac{M^2}{Q^2}\right) I\left(\frac{Q^2}{4M^2}\right) \right] \Bigg\} + \mathrm{O}(\gamma^2), \tag{4.22}$$

where

$$J(a) = \int_0^1 \frac{\mathrm{d}\xi}{\sqrt{1-\xi}} \frac{1}{(1+\xi a)} = \frac{1}{\sqrt{a(1+a)}} \ln \frac{\sqrt{1+a} + \sqrt{a}}{\sqrt{1+a} - \sqrt{a}},$$

$$I(a) = \int_0^1 \frac{\mathrm{d}\xi}{\sqrt{1-\xi}} \frac{\ln(1+\xi a)}{(1+\xi a)}$$
$$= \frac{1}{\sqrt{a(1+a)}} \left[-\frac{\pi^2}{6} - \tfrac{1}{2}\ln^2 \frac{\sqrt{1+a} + \sqrt{a}}{\sqrt{1+a} - \sqrt{a}} + \ln^2 \frac{\sqrt{1+a} - \sqrt{a}}{2\sqrt{1+a}} \right.$$
$$\left. + 2\,\mathrm{Li}_2\left(\frac{\sqrt{1+a} - \sqrt{a}}{2\sqrt{1+a}} \right) \right], \tag{4.23}$$

and Li_2 is the dilogarithm function

$$\mathrm{Li}_2(x) = -\int_0^x \frac{dz}{z} \ln(1-z)\,. \tag{4.24}$$

By inserting eq. (4.22) into (4.11) we thus obtain

$$4M^2\sigma_{2,\,1\text{-loop}}(\rho, Q^2/M^2; M^2/Q_0^2)$$
$$= \alpha\alpha_s^2\left[c(\rho, Q^2/4M^2) + \bar{c}(\rho, Q^2/4M^2)\ln M^2/Q_0^2\right], \tag{4.25}$$

with the $\rho \to 0$ limit

$$\bar{c}(0,a) = \tfrac{4}{3}C_A e_Q^2\left[\frac{1}{2a} + \left(1 - \frac{1}{4a}\right)J(a)\right],$$

$$c(0,a) = \tfrac{4}{3}C_A e_Q^2\left[\frac{5}{6a} + \left(\frac{13}{6} - \frac{5}{12a}\right)J(a) + \left(1 - \frac{1}{4a}\right)I(a)\right]. \tag{4.26}$$

Eqs. (4.25) and (4.26) generalize the results (1.2) and (1.5) taking into account the photon off-shellness. In particular from (4.26) we have

$$\bar{c}(0, Q^2/4M^2) \simeq \begin{cases} \tfrac{28}{9}C_A e_Q^2, & (Q^2 \ll M^2) \\ \tfrac{16}{3}C_A e_Q^2(M^2/Q^2)\ln Q^2/M^2, & (Q^2 \gg M^2) \end{cases}$$

$$c(0, Q^2/4M^2) \simeq \begin{cases} \tfrac{164}{27}C_A e_Q^2, & (Q^2 \ll M^2) \\ \tfrac{8}{3}C_A e_Q^2(M^2/Q^2)\ln^2 Q^2/M^2, & (Q^2 \gg M^2) \end{cases} \tag{4.27}$$

Finally, we can compute the total cross section by Q^2-integration of eq. (4.17). By taking into account the y-dependent kinematical limit $Q^2 > y^2m^2/(1-y)$, we find the K-factor

$$K_N^{(e)}\left(\frac{M^2}{m^2}\right) = \frac{\sigma_N^{(e)}(M^2/Q_0^2, M^2/m^2)}{\sigma_{\gamma g, N}(M^2/Q_0^2)}$$

$$= \frac{\alpha}{\pi}\int_0^1 \frac{dy}{y} y^N \int_{\frac{1}{2}-i\infty}^{\frac{1}{2}+i\infty} \frac{d\gamma}{2\pi i\gamma^2}\left(\frac{M^2}{y^2m^2}\right)^{\gamma} \frac{h^{(2)}(\gamma, \gamma_N)}{h(\gamma_N)}$$

$$= \frac{\alpha}{\pi N}\left[\frac{2}{N} + \ln\frac{M^2}{m^2} + \chi(\gamma_N) + \mathrm{O}\left(\frac{m^2}{M^2}\right)\right], \tag{4.28}$$

$$\chi(\gamma_N) \equiv \frac{\partial}{\partial\gamma}\ln h^{(2)}(\gamma,\gamma_N)\bigg|_{\gamma=0} = 2\ln 2 + \tfrac{3}{4}\sqrt{\pi} - \frac{5-3\gamma_N}{7-5\gamma_N} - \psi(1-\gamma_N), \tag{4.29}$$

showing that, as anticipated in eq. (4.8), the Q^2-integration is indeed dominated by the region $y^2m^2 < Q^2 < M^2$ which gives the large contribution $(2/N + \ln M^2/m^2)$. In particular the term $1/N^2$ in eq. (4.28) is due to the factor y^2 in the lower limit y^2m^2 for Q^2. Of course, if experimentally only some minimum value $Q^2_{\rm min}$ ($M^2 \gg Q^2_{\rm min} \gg m^2$) of the photon mass is accessible, eq. (4.28) has to be changed accordingly and becomes

$$\frac{\sigma_N^{(e)}\left(M^2/Q_0^2, M^2/Q^2_{\rm min}\right)}{\sigma_{\gamma g, N}\left(M^2/Q_0^2\right)} = \frac{\alpha}{\pi N}\left[\ln\frac{M^2}{Q^2_{\rm min}} + \chi(\gamma_N) + O\left(\frac{Q^2_{\rm min}}{M^2}\right)\right]. \quad (4.30)$$

4.3. EXTREME ENERGIES

In the opposite regime of extreme energies ($\alpha_s \ln 1/\rho \gg \ln M^2/Q_0^2$), the gluon anomalous dimension departs from the perturbative value, by saturating at $\gamma = 1/2$. By the same manipulations of sect. 3 we find the expression

$$4M^2\sigma_2\left(\rho, \frac{Q^2}{M^2}; \frac{M^2}{Q_0^2}\right) \simeq G\left(\rho', \frac{M^2}{Q_0^2}\right)\int_{\frac{1}{2}-i\infty}^{\frac{1}{2}+i\infty}\frac{d\gamma}{2\pi i\gamma}\left(\frac{M^2}{Q^2}\right)^{\gamma} h^{(2)}(\gamma, 1/2),$$
$$\rho' \equiv \frac{4M^2 + Q^2}{S} \ll 1, \quad (4.31)$$

to be compared with the one in (3.23) for photo-production. We see that, since $\gamma_N = 1/2$, the behavior of (4.17) for $Q^2 \gg M^2$ is dominated by $\gamma = 1/2$, thus providing the change of scale $M^2/Q_0^2 \to Q^2/Q_0^2$ in eq. (3.22). More precisely, the r.h.s. of (4.31) takes, by eq. (4.18) the form

$$\frac{4M^2\sigma_2(\rho, Q^2/M^2; M^2/Q_0^2)}{G(\rho', M^2/Q_0^2)} = h(1/2)\left[\frac{M^2}{Q^2} + \left(\frac{11}{12} - \frac{M^2}{Q^2}\right)\sqrt{\frac{4M^2}{Q^2}}\arctan\sqrt{\frac{Q^2}{4M^2}}\right]$$
$$\simeq \begin{cases} h(1/2), & (Q^2 \ll M^2) \\ h(1/2)\frac{11}{12}\pi\sqrt{M^2/Q^2}, & (Q^2 \gg M^2) \end{cases}. \quad (4.32)$$

This "K-factor" is to be compared with the perturbative one in eq. (4.22). The main difference arises in the kinematical region $Q^2 \gg M^2$. While the perturbative value (4.22) is of order M^2/Q^2, and contains corrections of relative order $(\alpha_s/N)\ln Q^2/M^2$, the asymptotic value in (4.32) is of order $\sqrt{M^2/Q^2}$. This implies that the resummation effect is much larger than for the photo-production case. In fact, it has to make up for the anomalous dimension $\bar{\gamma} = 1/2$ in the relative scale factor $(M^2/Q^2)^{1-\bar{\gamma}}$.

An interesting point to note is that the asymptotic formula (4.32) admits a smooth $M^2 \to 0$ limit, which is obtained by setting $\rho' \to Q^2/S = x_B$ and by using expression (3.22) for the structure function. We find

$$F_2(x_B, Q^2/Q_0^2) = \lim_{M^2 \to 0} \frac{Q^2}{4\pi^2\alpha}\sigma_2 = \frac{11\pi^2}{128}\alpha_s \sum_q e_q^2 G(x_B, Q^2/Q_0^2), \quad (4.33)$$

where the sum over the light quark charges $\Sigma_q e_q^2$ replaces the heavy flavour charge e_Q^2 of σ_2. The limit in eq. (4.33) is finite because the $k_\perp$'s involved in the asymptotic formula are large ($\gamma \simeq 1/2$) so that there is no need of a collinear cut-off for massless quarks. Eq. (4.33) provides *an effective point-like coupling* of the "perturbative pomeron" to DIS.

Finally, the ratio of total lepto- vs photo-production cross sections takes the form

$$\frac{\sigma^{(e)}(\rho, M^2/Q_0^2, M^2/m^2)}{\sigma_{\gamma g}(\rho, M^2/Q_0^2)}$$

$$\simeq \frac{\alpha}{\pi}\int_0^1 \frac{dy}{y} \frac{G(\rho/y, M^2/Q_0^2)}{G(\rho, M^2/Q_0^2)} \int_{\frac{1}{2}-i\infty}^{\frac{1}{2}+i\infty} \frac{d\gamma}{2\pi i\gamma^2}\left(\frac{M^2}{y^2m^2}\right)^\gamma \frac{h^{(2)}(\gamma, 1/2)}{h(1/2)}$$

$$= \frac{\alpha}{4\pi\bar{\alpha}_s \ln 2}\left[\frac{1}{2\bar{\alpha}_s \ln 2} + \ln\frac{M^2}{m^2} + O(1)\right], \quad (4.34)$$

where we have used the "perturbative pomeron" behaviour in eq. (3.22) to evaluate the y-integral.

It is interesting to note the enhancing double-log factor $\alpha_s^{-1} \ln M^2/m^2 \sim \ln M^2/\Lambda^2 \ln M^2/m^2$ in (4.34) (coming from the small Q^2 phase space) which can partly overcome at extreme energies the extra factor of α of the electromagnetic lepton coupling.

The constant term O(1) in eq. (4.34) cannot be reliably computed within our leading log approximation. This is because, due to the $1/N^2$ contribution in eq. (4.28), the constant term in eq. (4.34) is also affected by next-to-leading corrections to the photo-production cross section. A similar effect does not arise for the lepto-production cross section with a fixed (y-independent) resolution $Q^2_{\min}$ on the photon mass. From eq. (4.30) we get at asymptotic energies

$$\frac{\sigma^{(e)}(\rho, M^2/Q_0^2, M^2/Q_{\min}^2)}{\sigma_{\gamma g}(\rho, M^2/Q_0^2)} = \frac{\alpha}{4\pi\bar{\alpha}_s \ln 2}\left[\ln\frac{M^2}{Q_{\min}^2} + \chi(1/2) + O\left(\frac{Q_{\min}^2}{M^2}\right)\right], \tag{4.35}$$

where the function $\chi(\gamma)$ is defined in eq. (4.29).

The contribution $\chi(1/2)$ in (4.35) measures the effect of the photon off-shellness on the total cross section. This effect can be reproduced by the Weizsäcker–Williams approximation [17]

$$\sigma^{(e)}(\rho, M^2/Q_0^2; M^2/Q_{\min}^2) \simeq \frac{\alpha}{\pi}\int_0^1 \frac{\mathrm{d}y}{y}\sigma_{\gamma g}(\rho/y, M^2/Q_0^2)\ln\frac{M_{\mathrm{eff}}^2}{Q_{\min}^2}, \tag{4.36}$$

provided an appropriate effective mass M_{eff} is used. Comparing eqs. (4.35) and (4.36) in the asymptotic regime we find a large effective mass

$$M_{\mathrm{eff}}/M = \exp\left(\tfrac{1}{2}\chi(1/2)\right) \simeq 7.03, \tag{4.37}$$

due to the fact that $\chi(1/2) \simeq 3.90$. Note that the value of M_{eff} in the perturbative regime $\gamma \ll 1$ is, by (4.29), about a factor of 2 smaller than (4.37). This shows that the resummation effect in eq. (4.35) is large, even after factorization of the resummed photo-production cross section.

5. High-energy factorization in the hadro-production case

In this case we mostly discuss the kinematical configuration in which the heavy flavour pair is produced in the central rapidity region. Thus the production vertex, corresponding to the subprocess

$$g(k_1) + g(k_2) \to \overline{Q}(p_3) + Q(p_4), \tag{5.1}$$

occurs with small values of momentum fractions $\bar{z}_1$, z_2, the z's being the Sudakov parameters of the transferred momenta, defined as follows

$$k_1^\mu = \bar{z}_1 p_1^\mu + k_{1\perp}^\mu + z_1 p_2^\mu, \qquad k_2^\mu = z_2 p_2^\mu + k_{2\perp}^\mu + \bar{z}_2 p_1^\mu. \tag{5.2}$$

The analogous region in lepto-production was the one of small y and z_2, with a photon replacing the gluon $g(k_1)$.

High energy factorization gives rise for the hadro-production case to a formula which is a convolution in $\bar{z}_1$, z_2 and involves two transverse momenta $\mathbf{k}_1, \mathbf{k}_2$. In a

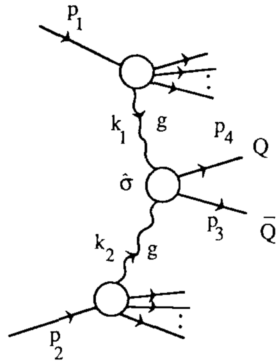

Fig. 9. Heavy flavour hadro-production in the central rapidity region at high energy.

more detailed form we write

$$4M^2\sigma^{(H)}(\rho, M^2/Q_0^2) = \int d^2\mathbf{k}_1 \int_0^1 \frac{d\bar{z}_1}{\bar{z}_1} \int d^2\mathbf{k}_2 \int_0^1 \frac{dz_2}{z_2} \mathscr{F}(\bar{z}_1, \mathbf{k}_1)$$

$$\times \hat{\sigma}_{gg}(\rho/\bar{z}_1 z_2, \mathbf{k}_1/M, \mathbf{k}_2/M) \mathscr{F}(z_2, \mathbf{k}_2), \qquad (5.3)$$

where the $\mathscr{F}$'s are the unintegrated gluon structure functions, defined in eq. (2.16), and $\hat{\sigma}_{gg}$ is obtained (fig. 9) by coupling the incoming gluons $g(k_1)$ and $g(k_2)$ to external partons with eikonal vertices.

The argument leading to the $k_\perp$-dependent factorization in eq. (5.3) is obtained, in a physical gauge with $n \cdot A = 0$ ($n^\mu = ap_1^\mu + bp_2^\mu$), by following the known analysis [7, 8] of gluon emission associated to small-x processes.

The emitted gluons are divided in two sets, (a) those $q_i^{(a)}$ essentially parallel to p_1, and (b) those $q_i^{(b)}$ essentially parallel to p_2. In the Sudakov parametrization

$$q_i^{(a)\mu} = \bar{y}_i^{(a)} p_1^\mu + q_{i\perp}^{(a)\mu} + y_i^{(a)} p_2^\mu, \qquad q_i^{(b)\mu} = y_i^{(b)} p_2^\mu + q_{i\perp}^{(b)\mu} + \bar{y}_i^{(b)} p_i^\mu, \qquad (5.4)$$

the two sets respectively correspond to (a) $\bar{y}_i^{(a)} \gg y_i^{(a)}$ and (b) $y_i^{(b)} \gg \bar{y}_i^{(b)}$, with $|q_{i\perp}^2| \ll S$. The gluons belonging, say, to set (b) are emitted by the system $\{p_1, q_i^{(a)}, p_3, p_4\}$ as a whole with a colour charge $\boldsymbol{T}_{k_2} = \boldsymbol{T}_{p_2} - \Sigma_i \boldsymbol{T}_i^{(b)}$, due to the coherence of large-angle QCD radiation [7]. Therefore, their emission can be factorized in sequence by the small-x effective current method [7, 8], building up the unintegrated structure function $\mathscr{F}(z_2, \mathbf{k}_2)$ obeying eq. (2.16).

Similar considerations hold for gluons in the set (a) and the function $\mathscr{F}(\bar{z}_1, \mathbf{k}_1)$. The remaining hard scattering vertex corresponds to the *bare* diagram in the process of fig. 9, i.e. the one without emitted gluons. The corresponding cross section is given by the high-energy limit of the $Q\bar{Q}$ contribution to $g(k_1, \mu_1) +$

$g(k_2, \mu_2) \to g(k_1, \nu_1) + g(k_2, \nu_2)$ imaginary part, i.e. by attaching eikonal couplings, as follows

$$\hat{\sigma}_{gg}\left(\frac{\rho}{\bar{z}_1 z_2}, \frac{\mathbf{k}_1}{M}, \frac{\mathbf{k}_2}{M}\right) \equiv \frac{\rho}{2\bar{z}_1 z_2} \frac{2\bar{z}_1^2 p_1^{\mu_1} p_1^{\nu_1}}{\mathbf{k}_1^2} \frac{2 z_2^2 p_2^{\mu_2} p_2^{\nu_2}}{\mathbf{k}_2^2} A_{\mu_1\nu_1,\mu_2\nu_2}(k_1, k_2). \quad (5.5)$$

We now go over to the analysis of the energy dependence of eq. (5.3) by use of ρ-moments and anomalous dimension integrals, as in sect. 3. This will allow us to discuss the resummation effects in the coefficient function and thus the corresponding "K-factor".

Two structure functions are involved in the factorization formula of eq. (5.3), so that we introduce two γ-integrals as follows

$$4M^2\sigma_N^{(H)}(M^2/Q_0^2) = \int d^2\mathbf{k}_1 \int d^2\mathbf{k}_2 \mathscr{F}_N(\mathbf{k}_1)\mathscr{F}_N(\mathbf{k}_2)\hat{\sigma}_{gg,N}(\mathbf{k}_1/M, \mathbf{k}_2/M)$$
$$= \int_{\frac{1}{2}-i\infty}^{\frac{1}{2}+i\infty} \frac{d\gamma_1}{2\pi i\gamma_1} \int_{\frac{1}{2}-i\infty}^{\frac{1}{2}+i\infty} \frac{d\gamma_2}{2\pi i\gamma_2} \left(\frac{M^2}{Q_0^2}\right)^{\gamma_1+\gamma_2} \left[1 - \frac{\bar{\alpha}_s}{N} f(\gamma_1)\right]^{-1}$$
$$\times \left[1 - \frac{\bar{\alpha}_s}{N} f(\gamma_2)\right]^{-1} h_N^{(H)}(\gamma_1, \gamma_2), \quad (5.6)$$

where $h_N^{(H)}$ is defined as in eq. (4.10) with $\hat{\sigma}_i$ replaced by $\hat{\sigma}_{gg}$. We can set again $N = 0$ in the hard vertex moments for $N \ll \gamma_i$ and $N \ll 1 - \gamma_1 - \gamma_2$, and accordingly we introduce the approximation

$$h_N^{(H)}(\gamma_1, \gamma_2) = h^{(H)}(\gamma_1, \gamma_2)(1 + O(N)), \qquad (N \ll \gamma_i, 1 - \gamma_1 - \gamma_2). \quad (5.7)$$

In the perturbative regime $\bar{\alpha}_s/N \ll 1$ we obtain a generalized factorization formula from the pole contributions at $\gamma_1 = \gamma_2 = \gamma_N$, i.e.

$$4M^2\sigma_N^{(H)}(M^2/Q_0^2) = \left[G_N(M^2/Q_0^2)\right]^2 h_N^{(H)}(\gamma_N, \gamma_N). \quad (5.8)$$

The resummation effects are embodied in the function $h^{(H)}$, that we have fully computed only for the abelian part (appendix C)

$$h^{(H)}(\gamma_1, \gamma_2) = h^{(ab)}(\gamma_1, \gamma_2) + h^{(nab)}(\gamma_1, \gamma_2), \quad (5.9)$$

$$h^{(ab)}(\gamma_1, \gamma_2) = \frac{\pi^2}{8N_c}\alpha_s^2 g(\gamma_1, \gamma_2), \quad (5.10)$$

where the function $g(\gamma_1, \gamma_2)$ is given in eq. (4.14). The small γ_i expansion of $h^{(H)}$ is also known from the single-$k_\perp$ hard vertex cross section $\hat{\sigma}_{gg}(\rho, \mathbf{k}/M, \mathbf{0})$ (appendix C)

$$h^{(H)}(\gamma_1, \gamma_2) \overset{\gamma_i \to 0}{\simeq} h^{(H)}(\gamma_1 + \gamma_2) = h^{(H)}(0)\left[1 + (\gamma_1 + \gamma_2)c^{(H)} + O(\gamma_i^2)\right], \quad (5.11)$$

where

$$h^{(H)}(0) = \frac{\pi}{N_c}\alpha_s^2\left(\frac{14}{9} - \frac{C_A}{C_F}\frac{11}{45}\right), \qquad h^{(H)}(0)c^{(H)} = \frac{\pi}{N_c}\alpha_s^2\left(\frac{82}{27} - \frac{C_A}{C_F}\frac{101}{675}\right). \quad (5.12)$$

From eqs. (5.8) and (5.11) one easily recovers the 1-loop perturbative results★ for hadro-production.

On the other hand, an interesting factorization test is obtained by replacing the structure function factor in eq. (5.8) by, e.g. the photo-production cross section, as follows

$$K_N^{(H)} = \frac{\sigma_N^{(H)}(M^2/Q_0^2)}{\left[\sigma_{\gamma g, N}(M^2/Q_0^2)\right]^2} = \frac{h^{(H)}(\gamma_N, \gamma_N)}{\left[h(\gamma_N)\right]^2}. \quad (5.13)$$

This ratio is largely independent of the unitarization effects discussed in ref. [9], which are tree-like and thus mostly affect the structure functions rather than the hard vertex. Thus, a detailed study of $h^{(H)}(\gamma_N, \gamma_N)$ will yield information on the energy-dependent resummation effects predicted by the factorization formula (5.3).

Some new peculiar feature appears for hadro-production at extreme energies. If the $Q\bar{Q}$ pair is produced in the central rapidity region and the energy is so large that $\bar{\alpha}_s \ln 1/\rho \gg \ln M^2/Q_0^2$, then *both* γ_1 and γ_2 drift towards the value $\gamma_1 = \gamma_2 = 1/2$. Thus $h^{(H)}(\gamma_1, \gamma_2)$ is evaluated close to the pole at $\gamma_1 + \gamma_2 = 1$ (or $\gamma_1 + \gamma_2 = 1 + N$ for $h_N^{(H)}$). This implies that the saddle point in γ_1, γ_2 has to be evaluated with more care, and one expects, qualitatively, a logarithmic enhancement of the cross section.

In order to understand this point, let us first note that the non-abelian part $h_N^{(nab)}$ is the most singular one close to $\gamma_1 + \gamma_2 = 1 + N$ and $\gamma_1 + \gamma_2 = 1$. This is

★ We agree with the results of Ellis and Ross in ref. [3], which correct a previous paper [18].

because, even for large $\mathbf{k}_1, \mathbf{k}_2$, the contribution of the gluon intermediate propagator is large and of the type

$$\hat{\sigma}_{gg}(\rho/\bar{z}_1 z_2, k_1/M, k_2/M) \simeq A_H(4M^2/s)\Theta(s-4M^2)$$

$$= \frac{4M^2 A_H}{\bar{z}_1 z_2 S - (\mathbf{k}_1+\mathbf{k}_2)^2}\Theta\left(\bar{z}_1 z_2 S - (\mathbf{k}_1+\mathbf{k}_2)^2 - 4M^2\right), \tag{5.14}$$

$$A_H = \frac{2\pi}{3}\frac{N_c}{N_c^2-1}\alpha_s^2, \tag{5.15}$$

in the region $M^2 \ll s \ll \bar{z}_1 z_2 S$. The pole part (5.14) contributes a logarithmic term to $\hat{\sigma}_{gg,N}$

$$\hat{\sigma}_{gg,N}(\mathbf{k}_1/M, \mathbf{k}_2/M) \simeq A_H\left(\frac{4M^2}{\mathbf{k}^2}\right)^{N+1}\ln\left(1+\frac{\mathbf{k}^2}{4M^2}\right), \qquad (\mathbf{k}=\mathbf{k}_1+\mathbf{k}_2), \tag{5.16}$$

which, for $M^2 \to 0$, has a collinear singularity responsible for the $Q\bar{Q}$ contribution to the running coupling constant.

Introducing (5.16) into the double $k_\perp$-transform of eq. (4.10) we obtain, from the region $M^2 \ll \mathbf{k}^2 \ll \mathbf{k}_1^2 \simeq \mathbf{k}_2^2$, the desired pole contribution

$$h_N^{(\mathrm{pole})}(\gamma_1,\gamma_2) = \frac{\gamma_1\gamma_2 A_H 4^{\gamma_1+\gamma_2}}{(N+1-\gamma_1-\gamma_2)^2(1-\gamma_1-\gamma_2)} \overset{\gamma_i\to 1/2}{\simeq} \frac{A_H}{N^2}\frac{1}{1-\gamma_1-\gamma_2}. \tag{5.17}$$

For comparison, we notice from eqs. (5.10) and (4.14) that the abelian part contributes still a single pole of the type $(N+1-\gamma_1-\gamma_2)^{-1}$.

We can now estimate the behaviour of $\sigma^{(H)}$ at extreme energies by evaluating the inverse Mellin transform of eq. (5.6) with the form (5.17) for $h_N^{(H)}$. By using the customary definitions $L = \ln S/4M^2$, $l = \ln M^2/Q_0^2$, and introducing a rapidity integration we first obtain the representation

$$4M^2\sigma^{(H)}(\rho, M^2/Q_0^2) = \int_0^L \mathrm{d}y \int_{\frac{1}{2}-i\infty}^{\frac{1}{2}+i\infty}\frac{\mathrm{d}\gamma_1}{2\pi i\gamma_1}\int_{\frac{1}{2}-i\infty}^{\frac{1}{2}+i\infty}\frac{\mathrm{d}\gamma_2}{2\pi i\gamma_2}\frac{A_H}{1-\gamma_1-\gamma_2}$$

$$\times \exp\left[\bar{\alpha}_s f(\gamma_1)y + \gamma_1 l + \bar{\alpha}_s f(\gamma_2)(L-y) + \gamma_2 l\right]. \tag{5.18}$$

We then perform saddle point integrations in γ_1 and γ_2, by taking into account the singular behaviour (5.17). The latter has the role of slowing down the approach of

γ_1 and γ_2 to the asymptotic values $\bar{\gamma}_i = 1/2$, so that for $\bar{\alpha}_s L \gg l$, one has

$$\delta_i = \tfrac{1}{2} - \bar{\gamma}_i \propto \frac{1}{\sqrt{\bar{\alpha}_s f''(1/2) L}} \equiv \delta . \tag{5.19}$$

Correspondingly, the expression (5.18) becomes asymptotically

$$\begin{aligned} 4M^2\sigma^{(H)}(\rho, M^2/Q_0^2) &\simeq \frac{1}{\bar{\alpha}_s f''(1/2)} \frac{\sqrt{2} A_H}{\pi\delta} \exp[\bar{\alpha}_s f(1/2 - \delta) L + l] \\ &\simeq \left[G(\sqrt{\rho}, M^2/Q_0^2)\right]^2 \frac{\pi L}{2} \frac{\sqrt{2e} A_H}{2[\bar{\alpha}_s f(1/2)]^2} \frac{1}{\pi\delta} . \end{aligned} \tag{5.20}$$

The last factor in eq. (5.20) is the logarithmic enhancement we were mentioning before. It represents, roughly, the multiplicity of large-$k_\perp$ gluons fragmenting in a $Q\bar{Q}$ pair. The latter contains, besides the $\pi L/2$ factor coming from rapidity integration, an additional large "K-factor"

$$\frac{\sqrt{2e} A_H \sqrt{\bar{\alpha}_s f''(1/2) L}}{2\pi[\bar{\alpha}_s f(1/2)]^2} , \qquad (f''(1/2) = 28\zeta(3)) , \tag{5.21}$$

coming from the $k_\perp$-integrations.

The physical interpretation of the large factor (5.21) comes from the large $k_\perp$-behaviour of the hard vertex cross section, quoted in eq. (5.16). As already noticed in sect. 3, the $(k_\perp^2)^{-1}$ decrease at fixed value of $S/k_\perp^2$ is a sign of the compositeness of the $Q\bar{Q}$ probe, which is capable of damping the $k_\perp$-integrals. However, with increasing anomalous dimension in the structure functions, the $k_\perp$-integrals eventually diverge, and $\gamma_1 = \gamma_2 = 1/2$ is precisely the situation when this first occurs.

The above remarks imply a word of caution as to the reliability of our resummation for hadro-production in the central region. The near divergence of the $k_\perp$-integrals is signalled in eq. (5.21) by its singular dependence on α_s, which cancels the perturbative factor of α_s^2 in A_H. On one hand, this implies that the actual value of the K-factor may be dependent on the details of the factorization scheme. For instance, introducing a running coupling constant $\alpha_s(\mathbf{k}^2)$ at the hard vertex may introduce log log factors in the result.

On the other hand the above singular behaviour may endanger the hierarchy of logarithms considered so far: sub-leading terms by one power of α_s can in principle be enhanced by more $k_\perp$-integrations, unless proved to be governed by the same K-factor. A better analysis of these points is left to future investigations.

6. Discussion

In this paper, we have systematically used the $k_\perp$-dependent factorization of the hard vertex and structure function terms due to Regge behaviour, in order to evaluate and resum the large perturbative contributions to the coefficient function of heavy flavour production. In the leading $\ln 1/\rho$ approximation, the hard vertex cross section is defined as the lowest order diagrams in figs. 2a, 7, 9 and is thus gauge invariant (appendix B) and calculable despite its off-shell dependence on one or two $k_\perp$'s of the incoming gluons (photons). In other words, this cross section is defined as the double Regge-gluon contribution to the six parton processes $\mathrm{A}+\mathrm{B}\to\mathrm{A}+\mathrm{B}+\mathrm{Q}+\overline{\mathrm{Q}}$ (fig. 10b), as explained in appendix B. The ensuing factorization formulas have been given in eq. (2.3) for photo-production and in eqs. (4.5) and (5.3) for lepto- and hadro-production.

We have discussed the effect of resummation on the energy dependence in the perturbative (eqs. (3.12), (4.11) and (5.8)) and in the asymptotic regime (eqs. (3.23), (4.32) and (5.20)). The coefficient function is given in terms of the h-functions, which are $k_\perp$-averages of the hard vertex cross sections and are dependent on the ρ-moment index N and on the gluon anomalous dimension $\gamma_N(\alpha_s)$. The resummation is particularly important in the small-N limit ($N \ll \gamma_N$), and provides in this case large factors compared to the naive renormalization group factorization at the collinear pole. The latter is recovered, as expected, in the "normal" situation $N \gg \gamma_N$, corresponding to $\rho \backsim O(1)$ and to the on-shell limit of the hard vertex cross section.

It appears therefore, that the $k_\perp$-dependent factorization approach extrapolates smoothly between the large-N situation, in which usual factorization holds, and the small-N case, in which it provides the resummation of the large $(\alpha_s/N)^k$ terms.

One may wonder what is the energy threshold above which the resummation effects are really large. We have argued that the transition to the asymptotic

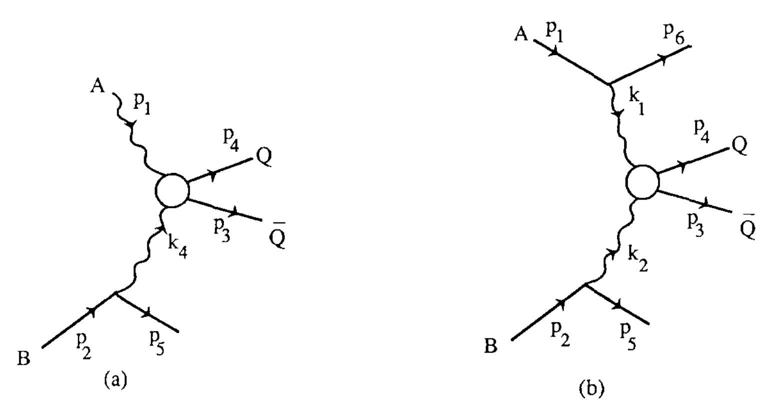

Fig. 10. (a) Five and (b) six parton processes for heavy flavour production in the high-energy limit.

regime occurs when $\bar{\alpha}_s \ln S/4M^2 = \ln M^2/Q_0^2$. Referring to the case of the bottom quark ($M \simeq 5$ GeV, $Q_0 \simeq 1$ GeV, $\Lambda \simeq 0.2$ GeV), this provides a value of $\rho \simeq 10^{-4}$. However, even before that value is reached, the resummed perturbative formulas in eqs. (3.9) and (4.13) provide well-defined enhancement factors in the coefficient function.

A different question is whether the large asymptotic K-factors so obtained (of order 5 for photo-production, logarithmically increasing for hadro-production) really provide an indication of the magnitude of the cross section compared to usual factorization formulas. Here one should note that at energies so large that $\bar{\alpha}_s \ln S/4M^2 \sim \ln M^2/Q_0^2$, also unitarization effects [10] not considered here are at work, which damp essentially the structure function factors in eqs. (3.23), (4.32), and (5.20). For this reason it is better to perform factorization tests by comparing two physical processes, so as to cancel the structure function factors, rather than taking the above expressions as absolute predictions.

We have followed this procedure systematically by comparing the lepto-production and photo-production processes. We find that their ratio still contains large resummation effects, both for the Q^2/M^2 dependence (eq. (4.32)) and for the total cross section (eq. (4.35)). This indicates that it is not actually possible to reduce the resummation effects in *all* K-factors by a proper definition of the structure functions. In fact, as we have emphasized in sect. 3, the actual values of the K-factors come from the detailed $k_\perp/M$ integrations which are in turn sensitive to the *form* of the hard vertex cross section. This effect is expected to be non-trivial for all *non-local* probes of the hard process, and in particular for the $Q\bar{Q}$ one considered here.

A final word of caution is needed concerning sub-leading terms. These are essentially due to gluon rescattering processes, either within the hard vertex (fig.

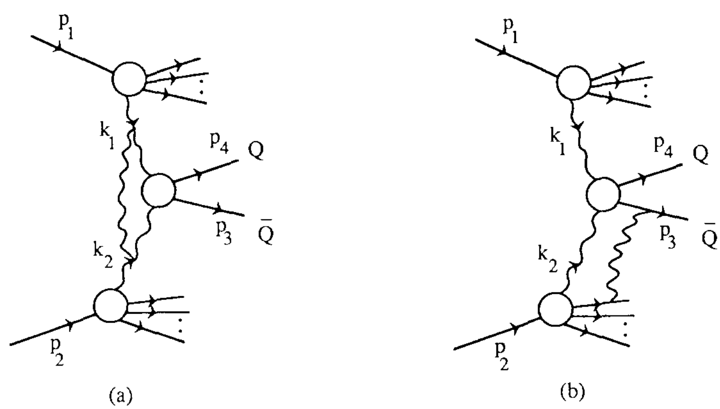

Fig. 11. Gluon re-scattering processes (a) within the hard vertex or (b) connecting it with the structure function.

11a), or connecting it with the structure function(s) (fig. 11b). Since all $k_\perp$'s are here of the order of the masses involved, there is no higher twist hierarchy in such rescattering diagrams. They are suppressed only by one power of $\alpha_s(M^2)$, because they miss one enhancing $\ln \rho$. Thus our approach has in general the same range of validity as the one for the small-x anomalous dimension [5]. However, some more care is needed in the hadro-production case (sect. 5) where one should check that the logarithmic enhancements due to the $k_\perp$-integrations do not spoil the hierarchy of the sub-leading contributions.

Appendix A

In this appendix we describe the kinematics for the hadro-production process in fig. 9. The simpler cases of photo-production (fig. 2) and lepto-production (fig. 7) can in turn be obtained by the identification

$$k_1^\mu \equiv p_1^\mu\,, \qquad k_2^\mu \equiv k^\mu\,, \quad \text{(photo-production)}\,, \tag{A.1}$$

$$k_1^\mu \equiv q^\mu = y p_1^\mu + q_\perp^\mu + \bar{y} p_2^\mu\,, \qquad q^2 = -Q^2\,, \quad \text{(lepto-production)}\,. \tag{A.2}$$

We work in the centre-of-mass frame of the incoming partons p_1, p_2

$$p_{1,2} = \tfrac{1}{2}\sqrt{S}\,(1, \mathbf{0}, \pm 1)\,, \qquad 2 p_1 \cdot p_2 = S\,, \tag{A.3}$$

and introduce the following Sudakov parametrization for the momenta of the exchanged partons k_1, k_2 and of the heavy quark p_4

$$k_1^\mu = \bar{z}_1 p_1^\mu + k_{1\perp}^\mu + z_1 p_2^\mu\,, \qquad z_1 = \frac{k_1^2 + \mathbf{k}_1^2}{\bar{z}_1 S}\,,$$

$$k_2^\mu = z_2 p_2^\mu + k_{2\perp}^\mu + \bar{z}_2 p_1^\mu\,, \qquad \bar{z}_2 = \frac{k_2^2 + \mathbf{k}_2^2}{z_2 S}\,,$$

$$p_4^\mu = (z_1 + z_2)\tau p_2^\mu + p_{4\perp}^\mu + (\bar{z}_1 + \bar{z}_2)\bar{\tau} p_1^\mu\,. \tag{A.4}$$

The longitudinal momentum fractions in eq. (A.4) have the following Lorentz invariant expressions

$$z_i = \frac{p_1 k_i}{p_1 p_2}\,, \qquad \bar{z}_i = \frac{p_2 k_i}{p_1 p_2}\,, \qquad (i = 1,2)\,,$$

$$\tau = \frac{p_1 p_4}{p_1(k_1 + k_2)}\,, \qquad \bar{\tau} = \frac{p_2 p_4}{p_2(k_1 + k_2)}\,. \tag{A.5}$$

The heavy flavour phase space is

$$d\Phi = \frac{d^4p_3}{(2\pi)^3}\frac{d^4p_4}{(2\pi)^3}\delta_+(p_3^2 - M^2)\delta_+(p_4^2 - M^2)(2\pi)^4\delta^{(4)}(p_3 + p_4 - k_1 - k_2). \tag{A.6}$$

By using the four-momentum conservation constraint and the heavy quark mass-shell condition in eq. (A.6), we can perform the integration over p_3 and $\bar{\tau}$ and we obtain

$$p_4^\mu = (z_1 + z_2)\tau p_2^\mu + p_{4\perp}^\mu + \frac{M^2 + \mathbf{p}_4^2}{(z_1 + z_2)\tau S}p_1^\mu,$$

$$p_3^\mu = (z_1 + z_2)(1-\tau)p_2^\mu + p_{3\perp}^\mu + \frac{M^2 + \mathbf{p}_3^2}{(z_1 + z_2)(1-\tau)S}p_1^\mu, \tag{A.7}$$

$$d\Phi = \frac{1}{8\pi^2}d^2\mathbf{p}_4\frac{d\tau}{\tau(1-\tau)}\Theta(1-\tau)\Theta(\tau)\Theta(z_1 + z_2)$$

$$\times\delta\left((z_1 + z_2)(\bar{z}_1 + \bar{z}_2)S - \mathbf{k}^2 - \frac{M^2 \pm \tilde{\mathbf{q}}^2}{\tau(1-\tau)}\right), \tag{A.8}$$

where we have defined the total transverse momentum $\mathbf{k}$

$$\mathbf{k} = \mathbf{k}_1 + \mathbf{k}_2 = \mathbf{p}_3 + \mathbf{p}_4, \tag{A.9}$$

and the transverse momentum variable $\tilde{\mathbf{q}}$

$$\tilde{\mathbf{q}} = \mathbf{p}_4 - \tau\mathbf{k} = (1-\tau)\mathbf{k} - \mathbf{p}_3 = (1-\tau)\mathbf{p}_4 - \tau\mathbf{p}_3. \tag{A.10}$$

Eq. (A.8) expresses the heavy flavour phase space in terms of the independent kinematical variables $\{\tau, \mathbf{p}_4\}$ or equivalently $\{\tau, \tilde{\mathbf{q}}^2, \varphi\}$, being φ the azimuthal angle between $\mathbf{k}$ and $\tilde{\mathbf{q}}$

$$\cos\varphi = \frac{\mathbf{k}\cdot\tilde{\mathbf{q}}}{|\mathbf{k}|\,|\tilde{\mathbf{q}}|}. \tag{A.11}$$

In the high-energy limit investigated throughout the paper, we can further introduce strong ordering in longitudinal momenta

$$z_2 \gg |z_1| \simeq \mathbf{k}_1^2/S\,,$$
$$\bar{z}_1 \gg |\bar{z}_2| \simeq \mathbf{k}_2^2/S\,, \tag{A.12}$$

and simplify all the kinematics accordingly. In particular the kinematical invariants for the subprocess $k_1 + k_2 \to p_3 + p_4$ become

$$s = (p_3 + p_4)^2 = \frac{M^2 + (\mathbf{p}_4 - \tau\mathbf{k})^2}{\tau(1-\tau)} \simeq \bar{z}_1 z_2 S - \mathbf{k}^2\,,$$
$$M^2 - t = M^2 - (k_1 - p_4)^2 \simeq \frac{1}{1-\tau}\left[M^2 + \tau(\mathbf{p}_4 - \mathbf{k})^2 + (1-\tau)(\mathbf{k}_1 - \mathbf{p}_4)^2\right],$$
$$M^2 - u = M^2 - (k_1 - p_3)^2 \simeq \frac{1}{\tau}\left[M^2 + (1-\tau)\mathbf{p}_4^2 + \tau(\mathbf{k}_2 - \mathbf{p}_4)^2\right]. \tag{A.13}$$

For heavy flavour photo-production (fig. 2), according to (A.1), we have $\bar{z}_1 = 1$, $z_1 = k_{1\perp} = 0$ and we define $z_2 \equiv z$. The formulas (A.13) simplify and in particular the longitudinal momentum fraction τ is directly related to the transferred momentum t

$$s = \frac{M^2 + \tilde{\mathbf{q}}^2}{\tau(1-\tau)} \simeq zS - \mathbf{k}^2\,,$$
$$M^2 - t = 2p_1 p_4 = z\tau S\,, \qquad M^2 - u = 2p_1 p_3 = z(1-\tau)S\,. \tag{A.14}$$

By integrating over the transverse momentum variable $\tilde{\mathbf{q}}^2$ of eq. (A.10), the phase space (A.8) becomes

$$d\Phi = \frac{1}{16\pi^2}\,\mathrm{d}\varphi\,\mathrm{d}\tau\,\Theta(\tau)\Theta(1-\tau)\Theta\left(\frac{z}{\rho} - \frac{1}{4\tau(1-\tau)} - \frac{\mathbf{k}^2}{4M^2}\right), \tag{A.15}$$

where we have used the high-energy approximation (A.12) and introduced the azimuthal angle φ of eq. (A.11).

In the lepto-production case (fig. 7) the incoming and outgoing leptons are massive. In the high-energy limit the lepton mass can always be neglected and the kinematic formulas given in this appendix are still valid with the following identification of the off-shell photon variables

$$k_1^\mu \equiv q^\mu , \qquad \bar{z}_1 \equiv y , \qquad k_{1\perp} \equiv q_\perp . \tag{A.16}$$

The only effect of the lepton mass is to provide a lower limit on the momentum transfer Q^2. Since $\mathbf{q}^2 = (1-y)Q^2 - y^2 m^2$, one has

$$Q^2 \geqslant \frac{y^2 m^2}{1-y} . \tag{A.17}$$

This constraint gives a physical cut-off on the collinear singularity $Q^2 \to 0$ associated to the lepton scattering.

Appendix B

The evaluation of the basic matrix elements, involved in the computation of heavy flavour cross sections at high energy, is performed in this appendix.

According to the factorization theorem discussed at length throughout the paper, all we need to compute is the tree-level amplitude $\mathscr{M}^{\mu_1\mu_2}(k_1, k_2; p_3, p_4)$ for the sub-process $k_1 + k_2 \to \overline{\mathrm{Q}}(p_3) + \mathrm{Q}(p_4)$ (fig. 8a) saturated by appropriate physical (eikonal) polarizations ϵ_i $(i = 1,2)$. Here k_1 and k_2 stand for incoming off-shell gluons and/or photons. After computing $\mathscr{M}^{\mu_1\mu_2}$, we can evaluate all the reduced hard cross sections $\hat{\sigma}$ involved in the $k_\perp$-factorization formulas and, as a by-product, we can obtain the high-energy limit of the matrix elements for any process "2 massless partons $\to \mathrm{Q} + \overline{\mathrm{Q}} + n$ massless partons" with $n = 1,2$. The latter can be used to evaluate differential distributions as well as be implemented in Monte Carlo event generators.

We start considering the subprocess $\mathrm{g}(k_1) + \mathrm{g}(k_2) \to \overline{\mathrm{Q}}(p_3) + \mathrm{Q}(p_4)$ in the high-energy limit (see notation in appendix A)

$$k_1^\mu = \bar{z}_1 p_1^\mu + k_{1\perp}^\mu , \qquad k_2^\mu = z_2 p_2^\mu + k_{2\perp}^\mu . \tag{B.1}$$

The corresponding tree-amplitude $\mathscr{M}^{\mu_1\mu_2}$ (fig. 8b) is given by

$$\mathscr{M}_{\mu_1\mu_2}(k_1, k_2; p_3, p_4) = d_{\mu_1\nu_1}^{(n)}(k_1) d_{\mu_2\nu_2}^{(n)}(k_2) \hat{\mathscr{M}}^{\nu_1\nu_2}(k_1, k_2; p_3, p_4) , \tag{B.2}$$

$$\hat{\mathscr{M}}^{\mu_1\mu_2}(k_1, k_2; p_3, p_4)$$

$$\equiv i g_s^2 \bar{u}(p_4) \left\{ \gamma^{\mu_1} \frac{1}{\not{k}_2 - \not{p}_3 - M} \gamma^{\mu_2} t^{a_1} t^{a_2} + \gamma^{\mu_2} \frac{1}{\not{p}_4 - \not{k}_2 - M} \gamma^{\mu_1} t^{a_2} t^{a_1} \right.$$
$$\left. - \gamma^\lambda \frac{d_{\lambda\rho}^{(n)}(k_1 + k_2)}{(k_1 + k_2)^2} \Gamma^{\rho\mu_1\mu_2}(-k_1 - k_2, k_1, k_2)[t^{a_1}, t^{a_2}] \right\} v(p_3) , \tag{B.3}$$

where u and v are the heavy flavour spinors, Γ is the three-gluon vertex

$$\Gamma^{\mu_1\mu_2\mu_3}(k_1,k_2,k_3) = g^{\mu_1\mu_2}(k_1-k_2)^{\mu_3} + g^{\mu_2\mu_3}(k_2-k_3)^{\mu_1} + g^{\mu_3\mu_1}(k_3-k_1)^{\mu_2}, \tag{B.4}$$

and, according to the factorization formulas (5.3) and (5.5), we have included in $\mathcal{M}$ the polarization tensors $d^{(n)}$ of the incoming off-shell gluons. Let us recall that we are working in an axial gauge $n \cdot A = 0$ with the gauge vector (a and b being arbitrary c-numbers)

$$n^{\mu} = ap_1^{\mu} + bp_2^{\mu}, \tag{B.5}$$

and the polarization tensor

$$d_{\mu\nu}^{(n)}(k) = -g_{\mu\nu} + \frac{n_{\mu}k_{\nu} + k_{\mu}n_{\nu}}{nk} - n^2\frac{k_{\mu}k_{\nu}}{(\bar{n}k)^2}. \tag{B.6}$$

Notice that within the one-parameter gauge we have chosen, we are able to verify the gauge invariance of the final results by checking their independence on the ratio a/b.

The amplitude $\mathcal{M}$, for the case where any incoming gluon $g(k_i)$ is replaced by a photon $\gamma(k_i)$, is obtained from eq. (B.3) by replacing the (non-abelian) colour matrix coupling $g_s t^a$ with the corresponding (abelian) electromagnetic one ge_Q ($g^2/4\pi = \alpha$).

For the high-energy limit we are interested in, the amplitude $\mathcal{M}_{\mu_1\mu_2}$ in eq. (B.2) has to be saturated with eikonal couplings due to the initial state partons p_1, p_2 (see eq. (5.5)). Thus we have to compute

$$\mathcal{M}^{(\mathrm{eik})}(k_1,k_2;p_3,p_4) = \frac{2\bar{z}_1 z_2 p_1^{\mu_1} p_2^{\mu_2}}{\sqrt{\mathbf{k}_1^2\mathbf{k}_2^2}}\mathcal{M}_{\mu_1\mu_2}(k_1,k_2;p_3,p_4)$$

$$= \frac{2\bar{z}_1 z_2 p_1^{\mu_1} p_2^{\mu_2}}{\sqrt{\mathbf{k}_1^2\mathbf{k}_2^2}} d_{\mu_1\nu_1}^{(n)}(k_1) d_{\mu_2\nu_2}^{(n)}(k_2) \hat{\mathcal{M}}^{\nu_1\nu_2}(k_1,k_2;p_3,p_4). \tag{B.7}$$

The evaluation of (B.7) and the corresponding squared amplitude is complicated (at least for the non-abelian case where naive Ward identities do not work) by the Lorentz algebra of the physical gauge calculation. We can get rid of such a complication since

$$\mathcal{M}^{(\mathrm{eik})}(k_1, k_2; p_3, p_4) = \frac{2k_{1\perp}^{\mu_1} k_{2\perp}^{\mu_2}}{\sqrt{\mathbf{k}_1^2 \mathbf{k}_2^2}} \hat{\mathcal{M}}_{\mu_1\mu_2}(k_1, k_2; p_3, p_4). \tag{B.8}$$

The result (B.8) follows from eq. (B.7) by noticing that (B.1) and (B.6) give

$$p_1^{\mu} d_{\mu\nu}^{(n)}(k_1) = (1/\bar{z}_1) k_{1\perp\nu}, \qquad p_2^{\mu} d_{\mu\nu}^{(n)}(k_2) = (1/z_2) k_{2\perp\nu}. \tag{B.9}$$

Moreover in eq. (B.8) the gauge dependence drops out in $\hat{\mathcal{M}}$, too. This is because, from eqs. (B.3) and (B.8), one has to evaluate

$$\begin{aligned} & k_{1\perp\mu_1} k_{2\perp\mu_2} \Gamma^{\mu_1\mu_2\rho}(k_1, k_2, -k_1 - k_2) d_{\lambda\rho}^{(n)}(k_1 + k_2) \\ & \quad = k_{1\perp\mu_1} k_{2\perp\mu_2} \Gamma^{\mu_1\mu_2\rho}(k_1, k_2, -k_1 - k_2)\left(-g_{\lambda\rho} + \frac{(k_1 + k_2)_\rho n_\lambda}{n(k_1 + k_2)} + \dots \right). \end{aligned} \tag{B.10}$$

The dots stand for gauge terms proportional to $(k_1 + k_2)^\lambda = (p_3 + p_4)^\lambda$ which give a vanishing contribution to $\hat{\mathcal{M}}$, due to the conservation of the heavy flavour current $J^\lambda(p_3, p_4) = \bar{u}(p_4)\gamma^\lambda v(p_3)$. Then the contribution $(k_1 + k_2)^\rho$ in (B.10), acting on the three-gluon vertex, gives (by Ward identity)

$$k_{1\perp}^{\mu_1} k_{2\perp}^{\mu_2} \left(g_{\mu_1\mu_2} k_1^2 - k_{1\mu_1} k_{1\mu_2} \right) - (k_1 \leftrightarrow k_2) = 0 \tag{B.11}$$

since $k_i^2 = -\mathbf{k}_i^2$. It follows that, in order to evaluate $\mathcal{M}^{(\mathrm{eik})}$, we can replace the polarization tensor $d_{\lambda\rho}^{(n)}$ in (B.3) by its Feynman gauge analogue $-g_{\lambda\rho}$ and the whole n-dependence in (B.8) has disappeared.

We ended up with a manifestly gauge invariant result for $\mathcal{M}^{(\mathrm{eik})}$. The reason for this is that the eikonal coupling induces physical polarizations for the incoming gluons, despite their off-shellness.

From now on the calculation is straightforward, although still cumbersome for the non-abelian term. The result we get for the squared amplitude is as follows

$$\mathscr{A}_{\mathrm{AB}}(k_1,k_2;p_3,p_4) = \overline{\sum}\left|\mathscr{M}_{\mathrm{AB}}^{(\mathrm{eik})}(k_1,k_2;p_3,p_4)\right|^2 = C_{\mathrm{AB}}\mathscr{A}^{(\mathrm{ab})}(k_1,k_2;p_3,p_4) + \overline{C}_{\mathrm{AB}}\mathscr{A}^{(\mathrm{nab})}(k_1,k_2;p_3,p_4), \tag{B.12}$$

$$\mathscr{A}^{(\mathrm{ab})}(k_1,k_2;p_3,p_4) = 4\left[\frac{(p_2k_1)(p_1k_2)}{(p_1p_2)^2}\right]^2\left\{\frac{(p_1p_2)^2}{(t-M^2)(u-M^2)} - \frac{1}{k_1^2k_2^2}\left[(p_1p_2) + 2\frac{(p_1p_4)(p_2p_3)}{t-M^2} + 2\frac{(p_1p_3)(p_2p_4)}{u-M^2}\right]^2\right\}, \tag{B.13}$$

$$\begin{aligned}\mathscr{A}^{(\mathrm{nab})}&(k_1,k_2;p_3,p_4)\\ &= \left[\frac{(p_2k_1)(p_1k_2)}{(p_1p_2)^2}\right]^2\left\{4(p_1p_2)^2\left[-\frac{1}{(t-M^2)(u-M^2)}\right.\right.\\ &\quad\left.-\frac{1}{s}\left(\frac{1}{t-M^2}-\frac{1}{u-M^2}\right)\left(\frac{p_1p_3}{p_1k_2}-\frac{p_2p_3}{p_2k_1}\right)+\frac{1}{s}\frac{(p_1p_2)}{(p_1k_2)(p_2k_1)}\right]\\ &\quad+\frac{2}{k_1^2k_2^2}\left[(p_1p_2)+4\frac{(p_1p_4)(p_2p_3)}{t-M^2}-\frac{\Delta}{s}\right]\\ &\quad\left.\times\left[(p_1p_2)+4\frac{(p_1p_3)(p_2p_4)}{u-M^2}+\frac{\Delta}{s}\right]\right\},\end{aligned} \tag{B.14}$$

where (appendix A) $t=(k_1-p_4)^2$, $u=(k_1-p_3)^2$, $s=(k_1+k_2)^2$ and we have defined

$$\Delta \equiv 2(p_1p_2)\left[2\frac{(p_1p_3)(p_2p_4)}{(p_1p_2)} - 2\frac{(p_1p_4)(p_2p_3)}{(p_1p_2)} - k_1^2\frac{(p_1p_4)}{(p_1k_2)} + k_2^2\frac{(p_2p_4)}{(p_2k_1)} + p_4(k_1-k_2)\right]. \tag{B.15}$$

In eq. (B.12) $\overline{\Sigma}$ denotes the sum and average respectively over final and initial state spin and colour degrees of freedom. We have also introduced the subscript AB in order to specify the type (gluon or photon) of incoming partons in the subprocess $\mathrm{A}(k_1)+\mathrm{B}(k_2)\to\overline{Q}(p_3)+Q(p_4)$. The only AB dependence in matrix elements $\mathscr{A}_{\mathrm{AB}}$ is in the colour factors $C_{\mathrm{AB}}, \overline{C}_{\mathrm{AB}}$

$$C_{\gamma\gamma} = 2g^4 e_Q^2, \qquad C_{\gamma g} = C_{g\gamma} = g_s^2 g^2 e_Q^2, \qquad C_{gg} = \frac{1}{2N_c} g_s^4, \tag{B.16}$$

$$\overline{C}_{gg} = \frac{1}{4}\frac{C_A}{C_F}\frac{g_s^4}{N_c} = \frac{N_c}{2(N_c^2-1)} g_s^4, \qquad \overline{C}_{\gamma\gamma} = \overline{C}_{\gamma g} = \overline{C}_{g\gamma} = 0. \tag{B.17}$$

The results (B.12)–(B.14) allow to compute the hadro-production cross section and σ_2 for the lepto-production process. In the photo-production case, only the incoming gluon k_2 is off-shell and coupled with the eikonal vertex. However, we notice that the corresponding matrix element can be obtained by (B.12) without further calculations of Feynman diagrams. The basic observation is as follows.

In order to compute the matrix element for the subprocess $\mathrm{A}(p_1) + \mathrm{B}(k_2) \to \overline{\mathrm{Q}}(p_3) + \mathrm{Q}(p_4)$ we have to replace k_1 with p_1 in eq. (B.3) for $\hat{\mathscr{M}}$ and then to evaluate the squared amplitude substituting $2k_{1\perp\mu_1}k_{1\perp\nu_1}/\mathbf{k}_1^2$ with $d^{(n)}_{\mu_1\nu_1}(p_1)$ in eq. (B.8). It is straightforward to verify the following identities

$$d^{(n)}_{\mu\nu}(p_1) = -g_{\mu\nu} + \frac{p_{1\mu}p_{2\nu} + p_{2\mu}p_{1\nu}}{p_1 p_2} \equiv -g^{(\perp)}_{\mu\nu}, \tag{B.18}$$

$$\left\langle \frac{2k_{1\perp\mu}k_{1\perp\nu}}{\mathbf{k}_1^2} \right\rangle_{\varphi_1} = -g^{(\perp)}_{\mu\nu}, \tag{B.19}$$

where $\langle\ \rangle_{\varphi_1}$ denotes average over the azimuthal angle φ_1 of $k_{1\perp}$. Therefore, the equivalence between eqs. (B.18) and (B.19) implies that the squared amplitude for the subprocess $\mathrm{A}(p_1) + \mathrm{B}(k_2) \to \overline{\mathrm{Q}}(p_3) + \mathrm{Q}(p_4)$ can be obtained from (B.12) by azimuthal average over φ_1 and performing the limit $\bar{z}_1 \to 1$, $k_{1\perp} \to 0$. The result we get is the following

$$\mathscr{A}_{\mathrm{AB}}(p_1, k_2; p_3, p_4) = C_{\mathrm{AB}}\mathscr{A}^{(\mathrm{ab})}(p_1, k_2; p_3, p_4) + \overline{C}_{\mathrm{AB}}\mathscr{A}^{(\mathrm{nab})}(p_1, k_2; p_3, p_4), \tag{B.20}$$

$$\mathscr{A}^{(\mathrm{ab})}(p_1, k_2; p_3, p_4) = \left(\frac{p_1 k_2}{p_1 p_2}\right)^2 \left\{ \frac{(p_2 p_3)^2 + (p_2 p_4)^2}{(p_1 p_4)(p_1 p_3)} - \frac{2M^2}{k_2^2}\left(\frac{p_2 p_4}{p_1 p_3} - \frac{p_2 p_3}{p_1 p_4}\right)^2 \right\}, \tag{B.21}$$

$$\begin{aligned}
&\mathscr{A}^{(\mathrm{nab})}(p_1, k_2; p_3, p_4) \\
&\quad = \left(\frac{p_1 k_2}{p_1 p_2}\right)^2 \left\{ \left(\frac{2(p_1 p_4)(p_2 p_3)}{s(p_1 p_2)} + \frac{2(p_1 p_3)(p_2 p_4)}{s(p_1 p_2)} - 1 \right) \right. \\
&\qquad \left. \times \frac{(p_2 p_3)^2 + (p_2 p_4)^2}{(p_1 p_4)(p_1 p_3)} - \frac{4M^2}{k_2^2}\left(\frac{2p_1 p_2}{s} - \frac{p_2 p_4}{p_1 p_3}\right)\left(\frac{2p_1 p_2}{s} - \frac{p_2 p_3}{p_1 p_4}\right) \right\},
\end{aligned} \tag{B.22}$$

where $s = (p_3 + p_4)^2$.

As a final check, the above limiting procedure can be in turn used for k_2 in order to obtain from (B.20) the known squared amplitude for the on-shell process $A(p_1) + B(p_2) \to \overline{Q}(p_3) + Q(p_4)$

$$\mathscr{A}_{AB}(p_1, p_2; p_3, p_4) = C_{AB}\mathscr{A}^{(ab)}(p_1, p_2; p_3, p_4) + \overline{C}_{AB}\mathscr{A}^{(nab)}(p_1, p_2; p_3, p_4), \tag{B.23}$$

$$\mathscr{A}^{(ab)}(p_1, p_2; p_3, p_4) = \frac{p_1 p_2}{(p_1 p_4)(p_1 p_3)} \left\{ \frac{(p_1 p_3)^2 + (p_1 p_4)^2}{p_1 p_2} + 2M^2\left(1 - \frac{M^2(p_1 p_2)}{2(p_1 p_4)(p_1 p_3)}\right)\right\}, \tag{B.24}$$

$$\mathscr{A}^{(nab)}(p_1, p_2; p_3, p_4) = -\frac{2}{(p_1 p_2)} \left\{ \frac{(p_1 p_3)^2 + (p_1 p_4)^2}{p_1 p_2} + 2M^2\left(1 - \frac{M^2(p_1 p_2)}{2(p_1 p_4)(p_1 p_3)}\right)\right\}. \tag{B.25}$$

The result described so far can be used to obtain the high-energy squared amplitudes for any process involving two massless partons in the initial state and one or two massless partons, besides the heavy flavour pair, in the final state. For the sake of conciseness we do not write down all the relevant matrix elements and we limit ourselves to give the rule to obtain such amplitudes.

Let us consider for instance the process $A(p_1) + B(p_2) \to \overline{Q}(p_3) + Q(p_4) + p_5$ (fig. 10a). According to the $k_\perp$-factorization theorem the corresponding squared amplitude is obtained by the one in eq. (B.20) for the subprocess $p_1 + k_2 \to p_3 + p_4$ times a factor of

$$4G_B \frac{1}{z_2^2 \mathbf{k}_2^2} = -4G_B\left(\frac{p_1 p_2}{p_1 k_2}\right)^2 \frac{1}{k_2^2}. \tag{B.26}$$

Here $G_B = (g^2, g_s^2 C_F, g_s^2 C_A)$ for $B =$ (electron, quark, gluon) respectively. A similar rule applies to the 6 parton process in fig. 10b.

Appendix C

This appendix is devoted to the detailed calculation of hard cross section factors and their N- and γ-moments.

C.1. PHOTO-PRODUCTION

The reduced cross section $\hat{\sigma}(\rho,\mathbf{k}^2/M^2)$ in eq. (2.15) is obtained by integration of the eikonal matrix element (B.20) over the $Q\bar{Q}$-phase space (A.15)

$$\hat{\sigma}(\rho/z,\mathbf{k}^2/M^2)=\int \mathrm{d}\Phi(\rho/2z)\mathscr{A}_{\gamma,\mathrm{g}}(p_1,k;p_3,p_4)\,. \tag{C.1}$$

Introducing the independent kinematical variables $\{\tau,\tilde{\mathbf{q}}^2,\varphi\}$ in eqs. (A.10),(A.11), we obtain

$$\mathscr{A}_{\gamma,\mathrm{g}}(p_1,k;p_3,p_4)=g_s^2g^2e_Q^2\left[\frac{\lambda_+^2+\lambda_-^2}{\tau(1-\tau)}+\frac{2M^2}{\mathbf{k}^2}\left(\frac{\lambda_+}{1-\tau}-\frac{\lambda_-}{\tau}\right)^2\right], \tag{C.2}$$

where we have defined

$$\lambda_+=(1-\tau)\left(1-\frac{\mathbf{k}^2}{zS}\right)+\frac{\tau\mathbf{k}^2}{zS}+\frac{2\tilde{\mathbf{q}}\cdot\mathbf{k}}{zS}\,,\qquad \lambda_-=1-\lambda_+\,. \tag{C.3}$$

Since the incoming photon $\gamma(p_1)$ is on-mass-shell, the matrix element (C.2) has a polynomial dependence of the angular variable $\cos\varphi$ in eq. (A.11) and the azimuthal integration over the angle φ is trivial. Using the mass-shell condition $\tilde{\mathbf{q}}^2+M^2=\tau(1-\tau)(zS-\mathbf{k}^2)$, a straightforward calculation gives the result (3.3) with the amplitude A_2 defined in eq. (3.6).

The computation of the reduced cross section $\hat{\sigma}(\rho,\mathbf{k}^2/M^2)$ now involves the remaining integral over the angular variable $\xi=4\tau(1-\tau)$

$$\hat{\sigma}(\rho,\mathbf{k}^2/M^2)=\frac{\rho}{16\pi}\int_0^1\frac{\mathrm{d}\xi}{\sqrt{1-\xi}}\Theta\left(\frac{1}{\rho}-\frac{1}{\xi}-\frac{\mathbf{k}^2}{4M^2}\right)A_2(\rho,\xi,\mathbf{k}^2/4M^2)\,. \tag{C.4}$$

Using the result

$$\int_{\xi_0}^1\frac{\mathrm{d}\xi}{\sqrt{1-\xi}}\,\frac{1}{\xi}=\ln\frac{1+\sqrt{1-\xi_0}}{1-\sqrt{1-\xi_0}}\,, \tag{C.5}$$

and the recurrence relation

$$(2n-1)\int_{\xi_0}^1\frac{\mathrm{d}\xi}{\sqrt{1-\xi}}\,\frac{1}{\xi^n}=2n\int_{\xi_0}^1\frac{\mathrm{d}\xi}{\sqrt{1-\xi}}\,\frac{1}{\xi^{n+1}}-\frac{2\sqrt{1-\xi_0}}{\xi_0^n}\,, \tag{C.6}$$

we obtain

$$\hat{\sigma}(\rho,\mathbf{k}^2/M^2) = 2\pi\alpha e_{\mathrm{Q}}^2\alpha_{\mathrm{s}}\Theta\left(\frac{1}{\rho}-1-\frac{k^2}{4M^2}\right)\rho\beta'\left\{\left[\left(1+\rho-\tfrac{1}{2}\rho^2\right)\mathscr{L}(\beta')-1-\rho\right]\right.$$

$$\left.+\left[8+\rho-(2+3\rho)\mathscr{L}(\beta')\right]\frac{\rho\mathbf{k}^2}{4M^2}+\left[-8+2\mathscr{L}(\beta')\right]\left(\frac{\rho\mathbf{k}^2}{4M^2}\right)^2\right\}, \quad \text{(C.7)}$$

$$\beta' \equiv \sqrt{1-\rho\left(1-\frac{\rho\mathbf{k}^2}{4M^2}\right)^{-1}}\,, \quad \text{(C.8)}$$

where $\mathscr{L}(\beta)$ is the bremsstrahlung function in eq. (1.4). In the on-shell limit $\mathbf{k}^2 = 0$, eq. (C.7) correctly reproduces the known result (1.1) for the photo-production cross section at the Born level [19].

In order to compute the N- and γ-moments of the reduced cross section, it is more convenient to start from the integral representation (C.4). To evaluate the $N = 0$-moment

$$\hat{\sigma}_{N=0}(\mathbf{k}^2/M^2) = \int_0^1 \frac{\mathrm{d}\rho}{\rho}\rho\int \mathrm{d}\Phi\, A_2(\rho,\xi,\mathbf{k}^2/4M^2), \quad \text{(C.9)}$$

we first perform the polynomial integration with respect to ρ

$$\hat{\sigma}_{N=0}(\mathbf{k}^2/M^2 = 4a) = \tfrac{2}{3}\pi\alpha_{\mathrm{s}}\alpha e_{\mathrm{Q}}^2\int_0^1 \frac{\mathrm{d}\xi}{\sqrt{1-\xi}}\left[\left(2-\frac{1}{a}\right)\frac{1}{1+\xi a}+\left(1+\frac{1}{a}\right)\frac{1}{(1+\xi a)^2}\right], \quad \text{(C.10)}$$

and then, using

$$J(a) = \int_0^1 \frac{\mathrm{d}\xi}{\sqrt{1-\xi}}\frac{1}{(1+\xi a)} = \frac{1}{\sqrt{a(1+a)}}\ln\frac{\sqrt{1+a}+\sqrt{a}}{\sqrt{1+a}-\sqrt{a}}\,,$$

$$\int_0^1 \frac{\mathrm{d}\xi}{\sqrt{1-\xi}}\frac{1}{(1+\xi a)^{n+1}} = \frac{1}{n(1+a)}\left[1+\frac{2n-1}{2}\int_0^1\frac{\mathrm{d}\xi}{\sqrt{1-\xi}}\frac{1}{(1+\xi a)^n}\right], \quad \text{(C.11)}$$

the ξ-integration gives

$$\hat{\sigma}_{N=0}(\mathbf{k}^2/M^2 = 4a) = \tfrac{4}{3}\pi\alpha_{\mathrm{s}}\alpha e_{\mathrm{Q}}^2\left[\frac{1}{2a}+\left(1-\frac{1}{4a}\right)J(a)\right]. \quad \text{(C.12)}$$

The hard cross section function

$$h(\gamma)=\gamma\int_0^\infty \frac{d\mathbf{k}^2}{\mathbf{k}^2}\left(\frac{\mathbf{k}^2}{M^2}\right)^\gamma \hat{\sigma}_{N=0}\left(\frac{\mathbf{k}^2}{M^2}\right) \tag{C.13}$$

is simply computed inserting the integral representation (C.10) into (C.13) and performing the $k_\perp$-integrals of the form

$$\int_0^\infty da \frac{a^\gamma}{(1+\xi a)^n}=\frac{1}{\xi^{\gamma+1}}B(1+\gamma,n-\gamma-1). \tag{C.14}$$

Then the final ξ-integration, evaluated in terms of Euler beta functions B, gives

$$h(\gamma)=\tfrac{2}{3}\pi\alpha_s\alpha e_Q^2 4^\gamma(7-5\gamma)B(1-\gamma,1+\gamma)B(1-\gamma,3/2), \tag{C.15}$$

or equivalently eq. (3.9).

C.2. LEPTO-PRODUCTION

We now consider the lepto-production cross section σ_2 in eqs. (4.2), (4.5). According to the factorization theorem (4.5), the reduced cross section $\hat{\sigma}_2$ is obtained by the eikonal matrix element (B.12)

$$\hat{\sigma}_2\left(\frac{\rho}{z_1 z_2},\frac{\mathbf{k}_1}{M},\frac{\mathbf{k}_2}{M}\right)=\int d\Phi \frac{\rho}{2 z_1 z_2}\mathscr{A}_{\gamma,g}(k_1,k_2;p_3,p_4), \tag{C.16}$$

$d\Phi$ being the phase space in eq. (A.8). Introducing the Sudakov variables defined in appendix A, we get

$$\hat{\sigma}_2\left(\rho,\frac{\mathbf{k}_1}{M},\frac{\mathbf{k}_2}{M}\right)=16\alpha_s\alpha e_Q^2\int d^2\mathbf{p}_4\int_0^1 d\tau\,\delta\left[M^2+(\mathbf{p}_4-\tau\mathbf{k})^2-\tau(1-\tau)\left(\frac{4M^2}{\rho}-\mathbf{k}^2\right)\right]$$
$$\times\frac{M^4}{\rho(t-M^2)(u-M^2)}\left\{1-\frac{[(\mathbf{k}_2^2-2\mathbf{p}_4\cdot\mathbf{k}_2)(\mathbf{k}_1^2-2\mathbf{p}_4\cdot\mathbf{k}_1)-2\mathbf{k}_1\cdot\mathbf{k}_2(M^2+\mathbf{p}_4^2)]^2}{\mathbf{k}_1^2\mathbf{k}_2^2(t-M^2)(u-M^2)}\right\} \tag{C.17}$$

In order to compute the lepto-production cross section σ_2 we are interested in the $N=0$-moment of $\hat{\sigma}_2$

$$\hat{\sigma}_{2,N=0}(\mathbf{k}_1/M,\mathbf{k}_2/M)=\int_0^1\frac{d\rho}{\rho}\hat{\sigma}_2(\rho,\mathbf{k}_1/M,\mathbf{k}_2/M). \tag{C.18}$$

Inserting (C.17) into (C.18), the ρ-integration can be performed using the mass-shell delta function and we obtain

$$\hat{\sigma}_{2,N=0}(\mathbf{k}_1/M, \mathbf{k}_2/M)$$

$$= 4\alpha_s \alpha e_Q^2 \int d^2\mathbf{p}_4 \int_0^1 \frac{d\tau}{\tau(1-\tau)} \frac{M^2}{\mathbf{k}_1^2\mathbf{k}_2^2} \frac{1}{(t-M^2)(u-M^2)}$$

$$\times \left\{ \mathbf{k}_1^2\mathbf{k}_2^2 - \frac{1}{(t-M^2)(u-M^2)} \left[(\mathbf{k}_2^2 - 2\mathbf{p}_4\cdot\mathbf{k}_2)(\mathbf{k}_1^2 - 2\mathbf{p}_4\cdot\mathbf{k}_1) \right.\right.$$

$$\left.\left. - 2\mathbf{k}_1\cdot\mathbf{k}_2(M^2+\mathbf{p}_4^2) \right]^2 \right\}. \quad (C.19)$$

The transverse momentum integration in eq. (C.19) is much more cumbersome than for the photo-production case. This is because for lepto-production the incoming partons k_1, k_2 are both off-shell and hence the denominators $(t - M^2)$ and $(u - M^2)$ have a non-trivial $k_\perp$ dependence. We can overcome this complication introducing into (C.19) the following Feynman parametrizations

$$\frac{1}{(t-M^2)(u-M^2)}$$

$$= \int_0^1 dy \frac{\tau(1-\tau)}{\left[M^2 + (\mathbf{p}_4 - \tau\mathbf{k}_2 - y\mathbf{k}_1)^2 + \tau(1-\tau)\mathbf{k}_2^2 + y(1-y)\mathbf{k}_1^2\right]^2},$$

$$\frac{1}{(t-M^2)^2(u-M^2)^2}$$

$$= \int_0^1 dy \frac{6\tau^2(1-\tau)^2 y(1-y)}{\left[M^2 + (\mathbf{p}_4 - \tau\mathbf{k}_2 - y\mathbf{k}_1)^2 + \tau(1-\tau)\mathbf{k}_2^2 + y(1-y)\mathbf{k}_1^2\right]^4}, \quad (C.20)$$

and performing the shift

$$\mathbf{p}_4 \to \mathbf{p} = \mathbf{p}_4 - (\tau\mathbf{k}_2 + y\mathbf{k}_1) \quad (C.21)$$

for the transverse momentum integration variable. The angular integrations over $\hat{\mathbf{p}}$

and the azimuthal angle φ_{12} between $\mathbf{k}_1$ and $\mathbf{k}_2$ are now trivial and we get

$$\begin{aligned}
&\hat{\sigma}_{2,N=0}(\mathbf{k}_1^2/M^2, \mathbf{k}_2^2/M^2) \\
&\quad \equiv \int_0^{2\pi} \frac{d\varphi_{12}}{2\pi} \hat{\sigma}_{2,N=0}(\mathbf{k}_1/M, \mathbf{k}_2/M) \\
&\quad = \pi\alpha\alpha_s e_Q^2 \int_0^1 \frac{d\xi_1}{\sqrt{1-\xi_1}} \int_0^1 \frac{d\xi_2}{\sqrt{1-\xi_2}} \int_0^\infty d\mathbf{p}^2 \frac{M^2}{\left[M^2 + \mathbf{p}^2 + \frac{1}{4}\xi_1\mathbf{k}_1^2 + \frac{1}{4}\xi_2\mathbf{k}_2^2\right]^2} \\
&\qquad \times \left\{ \left(1 - \tfrac{3}{4}\xi_1\xi_2\right) - \frac{3\xi_1\xi_2\left[(1-\xi_1)(1-\xi_2)\mathbf{k}_1^2\mathbf{k}_2^2 + \mathbf{p}^2\left((2-3\xi_1)\mathbf{k}_1^2 + (2-3\xi_2)\mathbf{k}_2^2 - 4M^2\right)\right]}{8\left[M^2 + \mathbf{p}^2 + \frac{1}{4}\xi_1\mathbf{k}_1^2 + \frac{1}{4}\xi_2\mathbf{k}_2^2\right]^2} \right\},
\end{aligned} \tag{C.22}$$

where we have defined $\xi_1 = 4y(1-y)$, $\xi_2 = 4\tau(1-\tau)$. The final $\mathbf{p}^2$-integration is of the form (C.14) and gives the integral representation (4.12).

The result (4.13), (4.14) for

$$h(\gamma_1, \gamma_2) = \gamma_1\gamma_2 \int_0^\infty \frac{d\mathbf{k}_1^2}{\mathbf{k}_1^2} \left(\frac{\mathbf{k}_1^2}{M^2}\right)^{\gamma_1} \int_0^\infty \frac{d\mathbf{k}_2^2}{\mathbf{k}_2^2} \left(\frac{\mathbf{k}_2^2}{M^2}\right)^{\gamma_2} \hat{\sigma}_{2,N=0}\left(\frac{\mathbf{k}_1^2}{M^2}, \frac{\mathbf{k}_2^2}{M^2}\right) \tag{C.23}$$

are obtained inserting (4.12) into (C.23), performing the $\mathbf{k}_i^2$-integrations according to

$$\int_0^\infty dx_1 \int_0^\infty dx_2 \frac{x_1^{\gamma_1} x_2^{\gamma_2}}{(1 + \xi_1 x_1 + \xi_2 x_2)^n} = \frac{\Gamma(1+\gamma_1)\Gamma(1+\gamma_2)\Gamma(n-\gamma_1-\gamma_2-2)}{\xi_1^{1+\gamma_1}\xi_2^{1+\gamma_2}\Gamma(n)}, \tag{C.24}$$

and evaluating the remaining ξ_i-integrations in terms of Euler beta functions.

We now describe the main steps involved in the calculation of the K-factor $K_N^{(2)}$ in eq. (4.18). According to eq. (4.17) we have to compute

$$K_N^{(2)}(Q^2/M^2) = \left(1 + \frac{Q^2}{4M^2}\right)^{-N} \int_{\frac{1}{2}-i\infty}^{\frac{1}{2}+i\infty} \frac{d\gamma}{2\pi i\gamma} \left(\frac{M^2}{Q^2}\right)^{\gamma} \frac{h(\gamma, \gamma_N)}{h(\gamma_N)}, \tag{C.25}$$

where $h(\gamma, \gamma_N)$ and $h(\gamma)$ are given in eqs. (4.13) and (3.9) respectively. Using eqs.

(4.14) and (C.15), we have

$$\frac{h(\gamma,\gamma_N)}{\gamma h(\gamma_N)} = \frac{\Gamma(5/2)}{(7-5\gamma_N)\Gamma(1-\gamma_N)} \frac{\Gamma(\gamma)\Gamma(1-\gamma)}{\Gamma(5/2-\gamma)} \times\left[(2+3\gamma_N-3\gamma_N^2)\Gamma(1-\gamma_N-\gamma)+(5-3\gamma_N)\Gamma(2-\gamma_N-\gamma)\right]. \tag{C.26}$$

Thus, inserting (C.26) into (C.25) and using the following integral representation for the hypergeometric function ($\mathrm{Re}\, c < \mathrm{Re}\,\alpha, \mathrm{Re}\,\beta$)

$$F(\alpha,\beta;\gamma;-z) = \frac{\Gamma(\gamma)}{\Gamma(\alpha)\Gamma(\beta)} \int_{c-i\infty}^{c+i\infty} \frac{\mathrm{d}t}{2\pi i} z^{-t} \frac{\Gamma(\alpha-t)\Gamma(\beta-t)\Gamma(t)}{\Gamma(\gamma-t)}, \tag{C.27}$$

we get

$$K_N^{(2)}\left(\frac{Q^2}{M^2}\right) = \left(1+\frac{Q^2}{4M^2}\right)^{-N} \frac{1}{7-5\gamma_N}\{(2+3\gamma_N-3\gamma_N^2)F(1,1-\gamma_N;5/2;-Q^2/4M^2) + (5-3\gamma_N)(1-\gamma_N)F(1,2-\gamma_N;5/2;-Q^2/4M^2)\}. \tag{C.28}$$

Using standard relations among hypergeometric functions, eq. (C.28) can be expressed in terms of the hypergeometric function

$$F\left(\tfrac{1}{2},1-\gamma;\tfrac{3}{2};\frac{z}{1+z}\right) = \tfrac{1}{2}(1+z)^{1-\gamma}\int_0^1 \frac{\mathrm{d}\xi}{\sqrt{1-\xi}} \frac{1}{(1+\xi z)^{1-\gamma}} \tag{C.29}$$

and we end up with eq. (4.18).

We conclude our calculations for the lepto-production cross section σ_2 noticing that its Born approximation $\hat{\sigma}_2(\rho, Q^2/M^2, \mathbf{k}_2^2/M^2 = 0)$ turns out to coincide by eq. (C.16) and the identification $Q^2 = \mathbf{k}^2$ with the photo-production off-shell cross section $\hat{\sigma}(\rho, \mathbf{k}^2/M^2)$ in (C.1). Thus the result (4.20) follows from eq. (C.7).

C.3. HADRO-PRODUCTION

The reduced hard cross section $\hat{\sigma}_{\mathrm{gg}}$ in eq. (5.3) is obtained, according to eq. (5.5), from the squared amplitude (B.12), as follows

$$\hat{\sigma}_{\mathrm{gg}}\left(\frac{\rho}{\bar{z}_1 z_2}, \frac{\mathbf{k}_1}{M}, \frac{\mathbf{k}_2}{M}\right) = \int \mathrm{d}\Phi \frac{\rho}{2\bar{z}_1 z_2} \mathscr{A}_{\mathrm{gg}}(k_1,k_2;p_3,p_4)$$

$$\equiv \hat{\sigma}_{\mathrm{gg}}^{(\mathrm{ab})}\left(\frac{\rho}{\bar{z}_1 z_2}, \frac{\mathbf{k}_1}{M}, \frac{\mathbf{k}_2}{M}\right) + \hat{\sigma}_{\mathrm{gg}}^{(\mathrm{nab})}\left(\frac{\rho}{\bar{z}_1 z_2}, \frac{\mathbf{k}_1}{M}, \frac{\mathbf{k}_2}{M}\right). \tag{C.30}$$

The abelian and non-abelian parts $\hat{\sigma}_{gg}^{(ab)}, \hat{\sigma}_{gg}^{(nab)}$ are defined according to the corresponding decomposition in (B.12) for the squared amplitude. Therefore, $\hat{\sigma}_{gg}^{(ab)}$ differs from the lepto-production cross section $\hat{\sigma}_2$ just by an overall coupling factor. From eq. (B.16) we get

$$\hat{\sigma}_{gg}^{(ab)}(\rho, \mathbf{k}_1/M, \mathbf{k}_2/M) = \frac{1}{2N_c} \frac{\alpha_s}{\alpha e_Q^2} \hat{\sigma}_2(\rho, \mathbf{k}_1/M, \mathbf{k}_2/M) \tag{C.31}$$

and the result (5.10) follows.

The hard cross section function $h^{(H)}(\gamma_1, \gamma_2)$ of eq. (5.9) is defined by

$$h^{(H)}(\gamma_1, \gamma_2) = \gamma_1 \gamma_2 \int \frac{d^2\mathbf{k}_1}{\pi \mathbf{k}_1^2} \left(\frac{\mathbf{k}_1^2}{M^2} \right)^{\gamma_1} \int \frac{d^2\mathbf{k}_2}{\pi \mathbf{k}_2^2} \left(\frac{\mathbf{k}_2^2}{M^2} \right)^{\gamma_2}$$

$$\times \int_0^1 \frac{d\rho}{\rho} \hat{\sigma}_{gg}(\rho, \mathbf{k}_1/M, \mathbf{k}_2/M) . \tag{C.32}$$

In the perturbative regime of small γ_i, this $k_\perp$-transform is dominated by the integration regions $\mathbf{k}_1^2 \gg \mathbf{k}_2^2$ and $\mathbf{k}_2^2 \gg \mathbf{k}_1^2$. In each of these regions we can neglect the dependence of $\hat{\sigma}_{gg}$ on the smallest transverse momentum and we obtain

$$h^{(H)}(\gamma_1, \gamma_2) \overset{\gamma_i \to 0}{\simeq} (\gamma_1 + \gamma_2) \int \frac{d^2\mathbf{k}_2}{\pi \mathbf{k}_2^2} \left(\frac{\mathbf{k}_2^2}{M^2} \right)^{\gamma_1 + \gamma_2} \int_0^1 \frac{d\rho}{\rho} \hat{\sigma}_{gg}(\rho, \mathbf{0}, \mathbf{k}_2/M)$$

$$\equiv h^{(H)}(\gamma_1 + \gamma_2) . \tag{C.33}$$

The single $k_\perp$-transform $h^{(H)}(\gamma_1 + \gamma_2)$ can be evaluated as for the photo-production case starting from the single-$k_\perp$ hard vertex cross section

$$\hat{\sigma}_{gg}\left(\frac{\rho}{z_2}, \mathbf{0}, \frac{\mathbf{k}_2}{M} \right) = \int d\Phi \, \frac{\rho}{2z_2} \mathscr{A}_{gg}(p_1, k_2; p_3, p_4) , \tag{C.34}$$

where $\mathscr{A}_{gg}(p_1, k_2; p_3, p_4)$ is the squared amplitude of eq. (B.20). A straightforward calculation gives the results in eqs. (5.11) and (5.12).

References

[1] R.K. Ellis and P. Nason, Nucl. Phys. B312 (1989) 551;
P. Nason, S. Dawson and R.K. Ellis, Nucl. Phys. B303 (1988) 607;
W. Beenakker, H. Kuijf, W.L. van Neerven and J. Smith, Phys. Rev. D40 (1989) 54

[2] G. Altarelli, M. Diemoz, G. Martinelli and P. Nason, Nucl. Phys. B308 (1988) 724

[3] R.K. Ellis and D.A. Ross, Fermilab preprint FERMILAB-Pub-90/19-T

[4] A. Bassetto, M. Ciafaloni and G. Marchesini, Phys. Rep. 100 (1983) 201

[5] L.N. Lipatov, Sov. J. Nucl. Phys. 23 (1976) 338;
E.A. Kuraev, L.N. Lipatov and V.S. Fadin, Sov. Phys. JETP 45 (1977) 199;
Ya. Balitskii and L.N. Lipatov, Sov. J. Nucl. Phys. 28 (1978) 6
[6] T. Jaroszewicz, Phys. Lett. B116 (1982) 291;
R. Kirschner, Z. Phys. C31 (1986) 135
[7] M. Ciafaloni, Nucl. Phys. B296 (1987) 249
[8] S. Catani, F. Fiorani and G. Marchesini, Nucl. Phys. B336 (1990) 18
[9] L.V. Gribov, E.M. Levin and M.G. Ryskin, Phys. Rep. 100 (1983) 1
[10] A.H. Mueller and J. Qiu, Nucl. Phys. B268 (1986) 427;
J.C. Collins and J. Kwiecinski, Nucl. Phys. B335 (1990) 89;
A.H. Mueller, Nucl. Phys. B335 (1990) 115;
E.M. Levin and M.G. Ryskin, Phys. Rep. 189 (1990) 268;
J. Bartels, G.A. Schuler and J. Blümlein, DESY preprint DESY-90-091;
E.M. Levin, G. Marchesini, M.G. Ryskin and B.R. Webber, Cavendish preprint Cavendish-HEP 90/9
[11] S. Catani, M. Ciafaloni and F. Hautmann, Phys. Lett. B242 (1990) 97
[12] S. Catani, M. Ciafaloni and F. Hautmann, Nucl. Phys. B (Proc. Suppl.) 18C (1990) 220, Cavendish preprint Cavendish-HEP 90/20, *in* Proc. Conf. QCD 90, Montpellier, July 1990, to appear
[13] J.C. Collins, D.E. Soper and G. Sterman, Nucl. Phys. B263 (1986) 37
[14] J.C. Collins and R.K. Ellis, Nucl. Phys. B (Proc. Suppl.) 18C (1990) 80
J.C. Collins, private communication
[15] J.C. Collins, D.E. Soper and G. Sterman, *in* Perturbative quantum chromodynamics, ed. A.H. Mueller (World Scientific, Singapore, 1989) and references therein
[16] A. Ali et al., in Proc. HERA Workshop, Hamburg 1987, ed. R.D. Peccei, p. 395
[17] G.A. Schuler, Nucl. Phys. B299 (1988) 21
[18] R.K. Ellis, Fermilab preprint FERMILAB-Conf-88/73-T, *in* Advanced research workshop on QCD hard hadronic processes, St. Croix, Virgin Islands, 1987
[19] L.M. Jones and H.W. Wyld, Phys. Rev. D17 (1978) 759